Chapter 6
Imaging Sensors

Abstract In the previous chapter, we described the location sensor under the CPS spectrum and the integration concept of GPS and INS sensors. It is said that the imagery data obtained by human eye accounts for 90% of total information acquired from various human sensory organs such as ear, nose and tongue. As the animals evolve from lower level (e.g. insects) to higher grade (e.g human), the utilization of visual data becomes higher. Likewise, as the substitution of natural intelligence by artificial intelligence advances, the dependence on imagery data increases. The underlying principle in data acquisition for CPS systems is to select imaging sensor suitable for operational application based on customer requirements and intended information such as training AI (Artificial Intelligence). An imaging sensor is a sensor converting the variable electromagnetic radiation delivered from the target into signals that convey the information. In order to identify the sensing requirements desired by the CPS instruments such as drones and self-driving cars, the pros and cons of various imaging sensors should be identified and utilized properly. Subsequently this chapter presented advantages and values of low-cost drone photography for hyper-localized targets (e.g. structural cracks in the skeleton of a concrete building and human hand gesture in the street crosswalk) in comparison to the existing methods.

6.1 Introduction

Image sensors used in electronic imaging devices include digital cameras, medical imaging equipment, night vision equipment, such as thermal imaging devices, radar, and others. Imaging sensor selection ultimately means meeting remote sensing requirements in the CPS systems design process, as it will make a great impact on product reliability. For any imaging sensor, the main categories of consideration will be the accuracy required, cost, size, reliability necessary, redundancy, energy consumption, and finally, the application at hand. There are a number of considerations in imaging sensor selection in optimising aerial data acquisition: navigation, flight restrictions, acceptable weather conditions, timing of flights during the day or

J.-S. Um, *Drones as Cyber-Physical Systems*,
https://doi.org/10.1007/978-981-13-3741-3_6

season, sun angle, ground spatial resolution, flying height, camera characteristics, ground coverage and image motion determination, which are all closely interrelated. Due to the relatively short history of drone remote sensing, there is no standardized comparison with traditional satellite or manned aircraft about determination of imaging sensor. The purpose of this chapter is to outline advantages and values of drone imaging sensor in comparison to the existing methods in the CPS framework and to introduce the related observation during the ortho-photo generation for hyper-localized target.

6.2 Four Sensor Selection Criteria

1. Spatial (what area and how detailed size)
2. Spectral (what colors – bands, wavelength sensitivity)
3. Temporal (how often, time of day/season/year)
4. Radiometric (how much deeper color depth)

The typical approach for sensor selection still depends on know-how acquired through experience. A wide array of remote sensors had developed to allow measurement of vegetation density, distance, and temperature, each specialised for a particular set of requirements. Given the large number of sensors on the market, the selection of a suitable sensor for a new application is a troublesome task for the person engaged in remote sensing. Although there are many factors to select remote sensor, the spatial, spectral, radiometric and temporal components of an image or set of images are recognized as fundamental (Table 6.1). Additionally, economic aspects and geometrical factors may be considered. These four selection criteria should always be interpreted by careful inter-comparison, as they have complementarity and interchangeability in image processing between standards. For example, if the spatial resolution is improved, larger-scale maps can be produced, but there is always a trade-off because it takes much more time and expense in image processing.

Table 6.1 Specification of representative satellite images based on sensor selection criteria

	Landsat 5 TM	IKONOS
Spatial resolution	30 m × 30 m	1 m × 1 m
Spectral resolution (unit: μm)	7 band	4 band
	1: 0.45–0.52 blue	1: 0.45–0.53 blue
	2: 0.52–0.60 green	2: 0.52–0.61 green
	3: 0.63–0.69 red	3: 0.64–0.72 red
	4: 0.76–0.90 Near IR	4: 0.77–0.88 Near IR
	5: 1.55–1.75 Middle IR	
	6: 10.4–12.5 Thermal IR	
	7: 2.08–2.35 Middle IR	
Temporal resolution	16 days	2 days
Radiometric resolution	8 bit	11 bit

6.3 Spatial Resolution

Spatial resolution refers to the size of the smallest possible feature that can be detected and the detail discernible in an image. It is most commonly expressed as the ground dimensions of an image cell. Only large features are visible in the coarse or low spatial resolution while small objects can be detected in fine or high spatial resolution images (Fig. 6.1). During an eye-sight check-up, the vision checklist is used to measure how well you see diverse sizes of the object in the same distance. That could be the example of investigating the spatial resolution of the human eye. Depending on how you look at it, the human eye can see 56 cm at 25 m. This means that human eye as remote sensor can perceive a depth difference of 0.1 cm at 1 m, 9 cm at 10 m, and 56 cm at 25 m. For instance, because the drone image is taken at very low altitude, it has a very fine spatial resolution.

Because commercial satellite imageries are taken at very high altitudes, they provide images with spatial resolutions ranging from a few meters to several km (Table 6.2). It is general that high spatial resolution imagery covers a narrow surface area. Until recently, the best commercially available pixel resolution from satellite imagery was 50 cm, but the US Government relaxed that restriction on 21 February 2015, and satellite companies can now legally distribute photos at about 25-cm resolution [1].

A spatial resolution changes as a reciprocal function (give and take) of several factors, including the platform height, the size of the sensor and the focal length of the lens. Cameras can be mounted on a variety of platforms including drone, ground-based stages, helicopters, aircraft, and spacecraft. The distance between

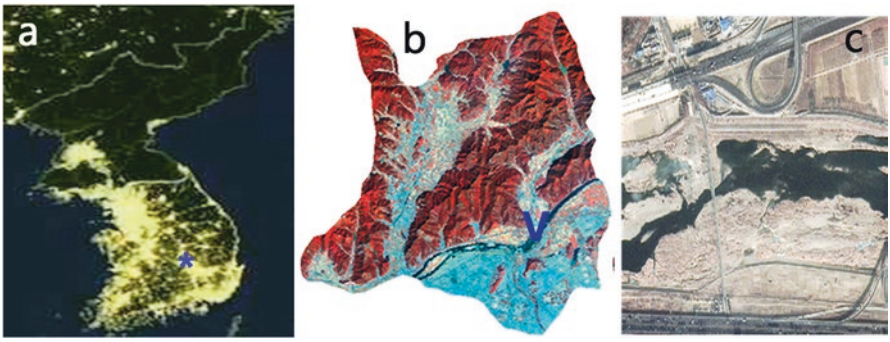

Fig. 6.1 A satellite imagery showing the level of information that is clearly distinguished according to different spatial resolution, (**a**) DMSP-OLS Nighttime satellite imagery (roughly 1 km spatial resolution) of Korean Peninsula, (**b**) Landsat Thematic Mapper scene (30 m spatial resolution) showing North district, Daegu metropolitan city, South Korea. Mountain and rivers are clearly recognizable. The magnified portion of site marked with * at the DMSP-OLS Nighttime satellite imagery (**a**), (**c**) IKONOS imagery (1 m spatial resolution), the magnified portion of site marked with V at the Thematic Mapper imagery (**b**), Smaller buildings and narrower streets are recognizable in the IKONOS image

Table 6.2 Spatial resolution of major remote sensing satellite imagery and corresponding mapping scale

Satellite	Spatial resolution (m)	Mapping scale
GeoEye-1	0.41 (0.31)	1/600 ~ 1/1200
GeoEye-2		
IKONOS	1 & 4	1/1200 ~ 1/2400
Quick Bird	0.82 & 3.2	1/1200 ~ 1/2400
KOMPSAT-3	0.7	1/1200 ~ 1/2400
IRS	5.8 & 22	1/2400 ~ 1/12,000
SPOT4	10 & 20	1/12,000 ~ 1/24,000
LANDSAT 5-8	30	1/24,000 ~ 1/50,000

the ground object and the remote platform has a crucial influence on the detail of information that can be collected. The camera at high altitudes will observe a larger area on the earth than at lower altitudes, but it does not see detailed features of the target (i.e. smaller scale). There is a big difference between satellite images and air-photos. The satellite sensors far away from their targets typically view a larger area (whole province or country), but couldn't distinguish individual houses. Sensors onboard aircraft flying over a city or town would be able to see individual buildings and cars, but would be viewing a much smaller area than the satellite sensor would [2].

6.3.1 Spatial Resolution, Pixel Size, and Scale

Remote sensing image of a digital format is composed of a matrix of picture elements, or pixels, which are the smallest units of an image. The pixel is commonly known as a raster, grid, cell or the square units. The spatial resolution and pixel size are often used interchangeably. In reality, they are not equivalent [3]. The spatial resolution is a measure of the smallest object that can be resolved by the sensor. An image sampled at a small pixel size does not necessarily have a high spatial resolution. It is difficult, however, to analytically determine the spatial resolution for the off-the-shelf UAV camera because the choice depends on many factors, including the sensor parameters, imaging optics (proper focusing), ISO range, atmospheric scattering, target motion and the human perception of image quality. However, it is often expressed that the resolution of a camera sensor used in the drone (e.g. CMOS built-in Zenmuse X3) is a function of the number of pixels and their size relative to the projected image. Therefore, it is often assumed that the smallest resolvable feature in any camera is equal to pixel size [4]. A small pixel size results in higher spatial resolution (higher spatial sampling).

If an imagery with a spatial resolution of 30 m is displayed with a surface area of 30 m per pixel, in this case, the spatial resolution and the pixel size have the same meaning [2]. However, by changing the computer monitor resolution, it is possible to display an image with a pixel size different from the original spatial resolution given from the sensor. The zoom application in the display monitor

does not increase spatial resolution of the original imagery. Satellite imagery posters of the Earth have the reduced number of pixels to represent larger areas within the limited paper space such as A3, although the original pixel size of the sensor remains the same. It is often the case that spatial resolution and scale are used as the same concept.

Spatial resolution, as the term itself implies, depends on the sensor because the sensor is capable of detecting the ground object in terms of size. The scale is a way of indicating how the ground distance is reduced on the map or in the photograph (Map Distance/Ground Distance), so it has nothing to do with the capabilities of the sensor. By utilizing remotely sensed imageries acquired from various sensors, it is possible to generate various scaled maps required by the user. When scanning aerial photographs, the user can specify the grid size of the image file, but the grid size determined by scanning process can not represent spatial resolution since user could not change capability of the sensor.

6.4 Spectral Resolution

The principle of remote sensing is based on the measurement of electromagnetic energy. The spectral resolution of a remote sensing system can be described as its ability to distinguish ground target in terms of measured wavelengths (Figs. 6.2 and 6.3). It is a specific wavelength range detected by a remote sensing instrument in the electromagnetic spectrum. This is typically defined in micrometers (Table 6.3). The sun emits various types of radiation and the human eye is only sensitive to the visible light portion in the electromagnetic spectrum of sunlight. Spectral resolution of human eyes as remote sensor is 0.4–0.7 μm since it can detect part of the visible spectrum. The human eye is insensitive to other solar radiation spectra, such as near infrared (NIR) and shortwave infrared (SWIR).

The visual systems of most animals are sensitive to visible wavelengths. Visible light (between 0.4 and 0.7 μm) is only one of many forms of electromagnetic energy.

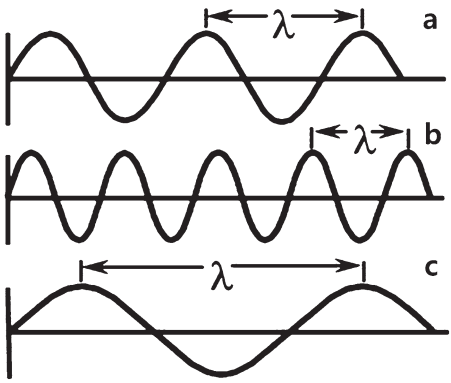

Fig. 6.2 Schematic representation of the inverse relationship involved in wavelength & frequency, (**a**) Near infrared (**b**) Red, (**c**) Microwave

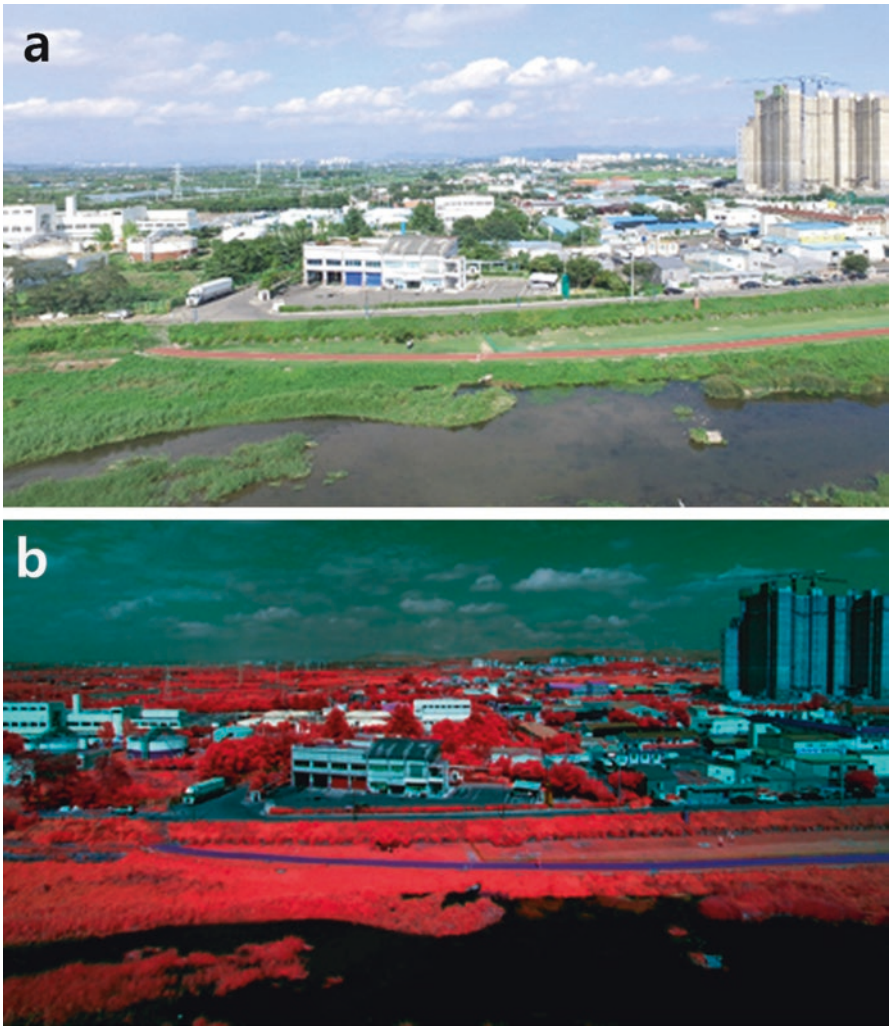

Fig. 6.3 Comparison of visible versus near-infrared imagery, (**a**) visible imagery containing information identical to the normal human perceptual range, (**b**) multi-spectral images including infrared. These are not images in the usual sense because the information represented is not directly visible to the human eye. Since the human eye cannot see infrared radiation, those wavelengths are displayed as a false color image. Green vegetation is displayed as reddish color, urban areas such as building are light blue-gray and clear or deep water is black

The sun is the most important source of electromagnetic energy on Earth. Remote sensing uses the radiant energy that is reflected and emitted from Earth at various wavelengths of the electromagnetic spectrum. The spectral signatures produced by wavelength-dependent sensor provide the key to discriminating different ground features in remote sensing image. Objects with significantly differentiated spectral characteristics such as water and vegetation, can be distinguished in a wide range of spectral signals, for instance, the visible and near infrared [5]. On the other hand,

Table 6.3 Spectral resolution of Landsat satellite imagery

Landsat 5	Landsat 7	Landsat 8
Band 1 Visible (0.45-0.52 μm) 30 m Band 2 Visible (0.52-0.60 μm) 30 m Band 3 Visible (0.63-0.69 μm) 30 m Band 4 Near-Infrared (0.76-0.90 μm) 30 m Band 5 Near-Infrared (1.5-1.75 μm) 30 m Band 6 Thermal (10.40-12.50 μm) 120 m Band 7 Mid-Infrared (2.08-2.35 μm) 30 m	Band 1 Visible (0.45-0.52 μm) 30 m Band 2 Visible (0.52-0.60 μm) 30 m Band 3 Visible (0.63-0.69 μm) 30 m Band 4 Near-Infrared (0.7-0.90 μm) 30 m Band 5 Near-Infrared (1.5-1.75 μm) 30 m Band 6 Thermal (10.40-12.50 μm) 60 m Low Gain/High Gain Band 7 Mid-Infrared (2.08-2.35 μm) 30 m Band 8 Panchromatic(PAN) (0.52-0.90 μm) 15 m	Nine spectral bands, including a pan band: Band 1 Visible (0.43-0.45 μm) 30 m Band 2 Visible (0.450-0.51 μm) 30 m Band 3 Visible (0.53-0.59 μm) 30 m Band 4 Red (0.64-0.67 μm) 30 m Band 5 Near-Infrared (0.85-0.8 μm) 30 m Band 6 SWIR (Short Wavelength Infrared) (1.57-1.65 μm) 30 m Band 7 SWIR 2 (2.1-2.29 μm) 30 m Band 8 Panchromatic (0.50-0.68 μm) 15 m Band 9 Cirus (1.36-1.38 μm) 30 m Thermal Infrared Sensor (TIRS) Band 10 TIRS 1 (10.6-1.19 μm) 10 m Band 1 TIRS 2 (1.5-12.51 μm) 10 m

less distinctive features in terms of spectral signatures, such as the extent of river water turbidity cannot be distinguished from a wide range of spectral signals. In order to detect such an object, a sensor having a finer spectral range is required.

Thus, we would require a sensor with higher spectral resolution. Two essential concepts of spectral resolution are described as the number of wavelength intervals ("bands") that are measured or narrow wavelength ranges (fine wavelength intervals) within a particular channel or band. Remote sensing image can be presented as a single very broad wavelength band (panchromatic), a few broad bands (multi-spectral), or many narrow wavelength bands (hyper-spectral), respectively. Black and white photography records the overall reflectance in wavelengths covering the entire visible portion of the electromagnetic spectrum. Its spectral resolution is fairly coarse, as the various wavelengths of the visible spectrum are not individually distinguished. Some satellite remote sensing systems record a single very broad band (referred to as a panchromatic band) to provide a synoptic overview of the scene, commonly at a higher spatial resolution than other sensors on board. SPOT satellites include a panchromatic band with a spectral range of 0.51–0.73 μm (green and red wavelength ranges) while NASA's Landsat 7 satellite includes a panchromatic band (a wider spectral range of 0.52–0.90 μm (green, red, and near infrared), with a spatial resolution of 15 m (on the contrary, 30-m for the multispectral bands).

In color photography, the sensor is also sensitive to the reflected energy over the visible portion of the spectrum. But it has a higher spectral resolution than that of black and white photography, as this is usually done by analyzing the spectrum of colors into three channels (red, green and blue). The remote sensing imagery gathered and stored from a narrow wavelength range is called as a channel, also sometimes referred to as a band. Spectral bandwidth is the width of an individual spectral channel with a narrow wavelength range in the remotely sensed imagery. As the spectral bandwidth narrows, the sensing ability for ground objects is improved. Each individual channel is sensitive to the reflected energy at the blue (short wavelengths), green (medium wavelengths), and red (long wavelengths) of the visible spectrum (Fig. 6.4). Red, blue, and green are the base colors of the visible light spectrum. This is called as basic color because we cannot create these colors by combining other colors. However, other colors such as yellow can be created by combining blue, green, and red at a certain ratio [5]. The longest visible wavelength is red and the shortest is violet. Sunlight includes electromagnetic waves of various wavelengths such as visible, ultraviolet and near-infrared portions of the spectrum.

For this reason, there are various electromagnetic waves around us, although they are invisible to human eyes. However, these electromagnetic waves can be detected by sensors of remote sensing instruments referred to as multi-spectral sensors. Multispectral images contain information outside the normal human perceptual range: this includes infrared, ultraviolet, X-ray or radar data (Table 6.4). An improved segmentation of objects can be achieved by combining an image captured on a visible light spectrum with an image taken in the thermal infrared (IR) spectrum. The visible light image is good for capturing color intensities while a thermal image, detects heat sources, such as warm bodies of people. Infrared region covers

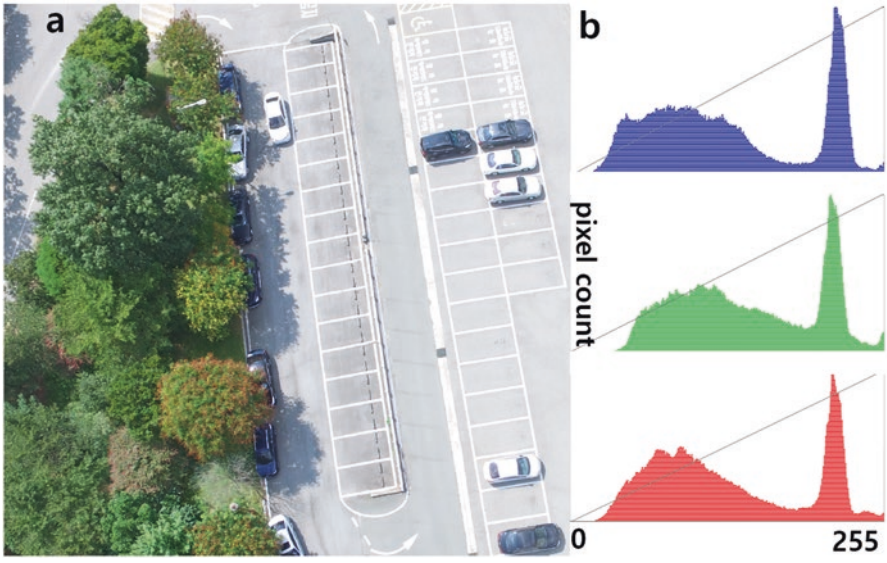

Fig. 6.4 Color digital image and RGB histogram, (**a**) color digital image (RGB combined channel) (**b**) RGB histogram

Table 6.4 Wavelength bands detected by remote sensing instruments

Band	Wavelength	Remarks
Ultraviolet (UV)	3 nm to 0.4 mm	Incoming UV radiation is absorbed by ozone in the upper atmosphere and atmospheric scattering is severe. So it is not employed in Remote Sensing.
Visible	0.4–0.7 μm	Violet: 0.4–0.446 μm
		Blue: 0.446–0.500 μm
		Green: 0.500–0.578 μm
		Yellow: 0.578–0.592 μm
		Orange: 0.592–0.620 μm
		Red: 0.620–0.7 μm
NIR- SWIR	0.7–3 μm	This is primarily reflected solar radiation and contains no information about thermal properties of materials.
		Commonly divided into the following regions:
		Near Infra Red (NIR) between 0.7 and 1.1 μm
		Middle Infra Red (MIR) between 1.3 and 1.6 μm .
		Short Wave Infra Red (SWIR) between 2 and 2.5 μm
Thermal IR	3–5 mm	Thermal infrared energy is emitted from all objects that have a temperature greater than absolute zero.
	8–14 mm	
Microwave	0.3–300 cm	These longer wavelengths can penetrate clouds and fog. Imagery may be acquired in the active or passive mode.
Radar	0.3–300 cm	Active mode of microwave remote sensing

an electromagnetic wave range of approximately 0.7–100 μm. It covers more than 100 times as wide as the visible portion. Infrared regions are divided into two categories according to their radiation properties: the reflected IR, and the emitted or thermal IR. Radiation in the reflected IR region has characteristics similar to that of the visible portion in remote sensing. The reflected IR has a wavelength range of approximately 0.7–3.0 μm which is slightly longer than visible light. The thermal IR region has properties that are different from visible and reflected IR portions because this energy is essentially the radiation that is emitted from the Earth's surface in the form of heat. The thermal IR region is located at approximately 3.0–100 μm wavelengths [5].

Spectral response curves characterize the reflectance patterns of a feature or target over a variety of wavelength range. The spectral reflectance of different ground targets can be measured in the laboratory or in the field, providing reference data that can be used to interpret images. Figure 6.5 shows contrasting spectral reflectance curves for three very common natural materials: dry soil, green vegetation, and water. The reflectance of dry soil rises uniformly through the visible and near infrared wavelength ranges, peaking in the middle infrared range. Reflectance pattern of green vegetation is relatively low in the visible range, but is higher for green light than for red or blue, producing the green color we see. The most noticeable feature of the vegetation spectrum is the dramatic rise in reflectance across the visible-near infrared boundary, and the high near infrared reflectance. Deep clear water bodies effectively absorb all wavelengths longer than the visible range, which results in very low reflectivity for infrared radiation [6].

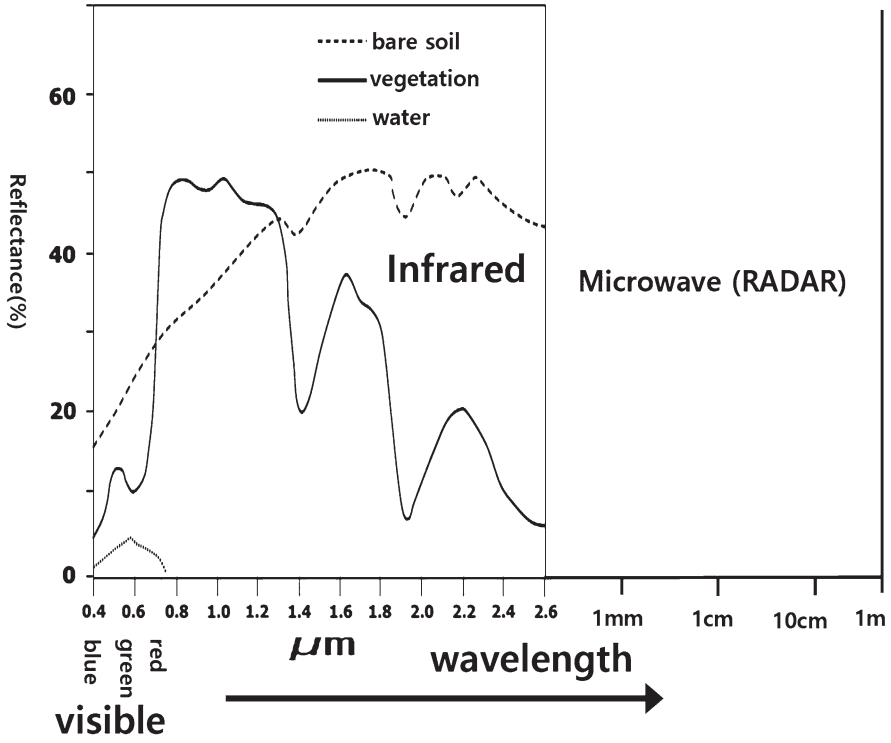

Fig. 6.5 Spectral response curves characterizing the reflectance patterns of a representative feature over a variety of wavelength range

There are two types of remote sensing: the optical (passive) and the microwave (active) system. Passive remote sensing uses the radiation emitted or reflected by an object when the sun is illuminating the Earth. In the passive remote sensing, observations can only take place when EMR (electromagnetic radiation) is naturally available. The reflected energy (visible, NIR near-infrared, MIR middle infrared or SWIR spectrum) is not available at night since the sun as naturally occurring energy source is not existing. However, energy that is naturally emitted (such as thermal infrared) from the target objects can be detected day or night. Thermal radiation (TIR) does not behave similarly to the visible light since it is emitted radiation from target objects. In the thermal radiation of the FIR (far-infrared) spectrum, the pedestrians, animals and automotive vehicles in use appear very clear at night since they show a relatively higher temperature than the surrounding environment although the sun is not available.

The sensor in active remote sensing transmits its own energy (e.g. a microwave radio signal) towards a target and detects the backscattered radiation. The biggest advantage of active sensor is that it can obtain remote sensing data anytime, regardless of the time of day or season (independent from weather and solar illumination effects). Radar (RAdio Detection And Ranging) remote sensing uses a backscattered

signal of microwave electromagnetic radiation to discriminate different targets. The time delay between the transmitted and reflected signals determines the distance (or range) to the target. Surveying & mapping professionals have been using both photogrammetry and LiDAR for survey purposes for a long time (Table 6.5). LiDAR is inherently more accurate and more expensive than photogrammetry. Photogrammetry is more visually appealing since photogrammetry's point cloud (known points in a coordinate system) has a RGB value for each point. But LiDAR point clouds colorized with ortho-photos never look natural as the photogrammetry point cloud. But of the two, LiDAR is the only technology that can penetrate a tree canopy to create high resolution DTM (Digital Terrain Model) or map complex structures application to require extreme vertical accuracy at night [7].

Advanced multi-spectral sensors called hyper-spectral sensors, detect hundreds of very narrow spectral bands throughout the visible, near infrared, and mid-infrared portions of the electromagnetic spectrum. The distinction between hyper and multispectral is sometimes based on an arbitrary "number of bands" or on the type of measurement, depending on what is appropriate to the purpose [8]. The hyperspectral imaging measures continuous (e.g. 400–1100 nm in steps of 0.1 nm) spectral range, as opposed to multispectral imaging which measures spaced (e.g. 400–1100 nm in steps of 20 nm) spectral bands [8]. A sensor with only 20 bands can also be hyper-spectral when it covers the range from 500 to 700 nm with 20 bands each 10 nm wide. But a sensor with 20 discrete bands covering the VIS, NIR, SWIR, MWIR, and LWIR would be considered multispectral [9]. Certain objects leave

Table 6.5 Comparison of LiDAR versus Photogrammetry

	LiDAR	Photogrammetry
Energy source	Active	Passive
Measurement tool	Light, lasers	Photographs
Cost	Expensive	Cheap
Visually appealing	No	Yes
Type of sensor	The main parameter of aerial laser scanning is the point density, which is expressed as the point number per square meter.	Frame or line scanning
Method to measure elevation	Only a single ray	Derive elevation by triangulating two different images of the same area
Imaging capability	Often image is not available.	High quality spatial and radiometric resolution image
Vertical accuracy	When extreme vertical accuracy (e.g. 10–15 cm) is required, LiDAR is better.	Dependent on flight altitude and the camera's focal length
End-lap and side-lap	Do not consider overlap. It does not provide overlapped imagery.	Overlap is required.
Independence from weather and solar illumination	It is less influenced by weather such as cloud conditions, seasons, and sun.	Shooting only on a clear day

unique 'fingerprints' in the hyper-spectral electromagnetic spectrum. For example, a hyper-spectral signature for river water helps water quality surveyor find source of water pollutants such as a specific textile manufacturing factory.

6.5 Radiometric Resolution

The radiometric resolution of remote sensors describes its ability to subdivide the energy received by a sensor into a number of discrete levels (recorded as integer values). The radiometric resolution means the sensitivity of a sensor to the electromagnetic energy received from targets. The very high radiometric resolution facilitates fine discrimination between different targets based on their numerical EMR (Electromagnetic Radiation) values in each of the narrow bands (Fig. 6.6). Human eye can discriminate about 30 shades of B/W (black and white image), thus its radiometric resolution is 30 for B/W image and 100 or so for colors. All modern imaging systems use some form of electronic sensor. An image from an electronic sensor array consists of a two-dimensional rectangular grid of numerical values that represent different radiometric levels.

The radiometric resolution is expressed in a range of grey tones, with black representing a digital number of 0 and, white representing the maximum value (for example, 255 in 8-bit data). This range corresponds to the number of bits used for coding numbers in binary format. Each bit records an exponent of a selected power 2 (e.g. 1 bit = 2). The maximum number of brightness levels available depends on the number of bits used in representing the energy recorded. Thus, if a sensor used 8 bits to record the data, there would be $2^8 = 256$ digital values available, ranging from 0 to 255. However, if only 4 bits were used, then only $2^4 = 16$ values ranging from 0 to 15 would be available. By comparing a 2-bit image with an 8-bit image, we can see that there is a large difference in the level of detail discernible depending on their radiometric resolutions [5].

Normal sensors have a gray scale of 6–8 bits. It is known that a gray scale of 10 bits or more is required to interpret the detailed features such as a shadow of a building. Many current satellite systems quantize data into 256 levels (8 bits of data in a binary encoding system). Landsat 7 has a radiometric resolution of 8 bits, IRS has 6 bits, and IKONOS has a radiometric resolution of 11 bits. The thermal infrared bands of the ASTER sensor are quantized into 4096 levels (12 bits). The narrower the band width of a specific spectral wavelength, the more detailed features within the specified electromagnetic wavelength can be detected. The radiometric resolution is increased as the ability to refining the physical quantity in a specific spectral wavelength is expanded. This can be said that the radiometric resolution is the performance of a sensor that differentiates the distribution range of numerical EMR values within narrow wavelengths.

The radiometric resolution of the Landsat 8 satellite is 12 bits, which is better than the 8 bits of Landsat 7, so that more precise radiant energy values can be recorded. As shown in Fig. 6.6a, pixel values in 8-bit data of Landsat 7 are defined

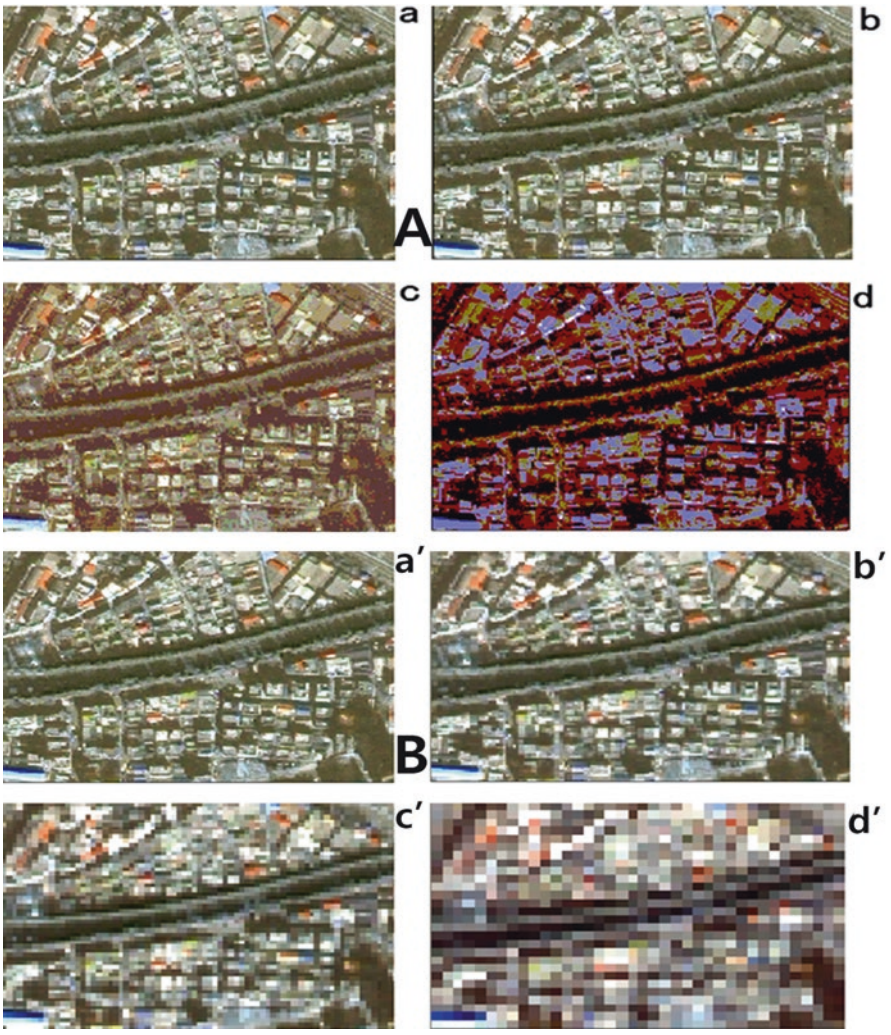

Fig. 6.6 Comparison of radiometric resolution versus spatial resolution. (**A**) Ground object definition changing according to radiometric resolution, a: higher radiometric resolution (16 bit), b: imagery (8 bit) degrading radiometric resolution from a imagery, c: imagery (4 bit) degrading radiometric resolution from b imagery, d: imagery (2 bit) degrading radiometric resolution from c imagery, (**B**) Ground object definition changing according to spatial resolution, a': higher (finer) spatial resolution (1 m), b': imagery (2 m) degrading spatial resolution from a' imagery, c': imagery (4 m) degrading spatial resolution from b' imagery, d': imagery (8 m) degrading spatial resolution from c' imagery

as minimum 0 to maximum 255 within a particular wavelength band. The maximum value of the Landsat 8 OLI sensor is 65,536 (256 * 256). This is because the 12 bit raw data of Landsat 8 OLI sensor is converted to 16 bits and distributed in comparison with the previous 8 bit Landsat imagery. The maximum value of Landsat 8 OLI

sensor (20427) in Fig. 6.6b means that they have a radiometric resolution converted to a 16bit. When analog image is scanned, the gray level of the image can be specified by the user, but the radiometric resolution is not determined in this process. Likewise, the radiometric resolution cannot be improved by the operation using the software later on. The radiometric resolution of the image depends on the ability of the sensor, thus that radiometric resolution of image taken by the Landsat 8 OLI sensor is still 12 bits (not a 16bit). Since the radiometric resolution is defined as the number of signals that can be distinguished, it becomes an important factor in identifying spatial objects.

Six bits (64 levels), 8 bits (256 levels) and 10 bits (1024 levels) are mainly used to express the degree or amount of information detected by each wavelength band. As a result, the higher the radiometric resolution, the higher degree to which the characteristics of ground objects can be determined. It can be said that designating the subdivision range of color displayed on a computer monitor such as 32 bits or 256 colors (that is, 8 bits) is a process that applies a concept similar to radiometric resolution. In the case of 4 bits, the monitor color tone can be divided into 16 kinds and displayed while in the case of 8 bits, it is possible to display the different color levels corresponding to 256. It is one of the most important performance indicators that any remote sensor must measure the signal from the ground target with enough precision to record details in the spectrum. In remote sensing, the ratio of the output signal (response amount) from an object on the surface of the earth and the output signal caused by other factors than those from the ground object surface is called S/N ratio (signal to noise ratio). The S/N is dependent on the detector sensitivity, the spectral bandwidth, and the intensity of the light reflected or emitted from the surface being measured. The higher the S/N ratio means the better the radiometric resolution. The same terminology is used in various electronic devices, such as a telephone, a camera, a radio, and a television, and this is one of the most important performance indicators of IT equipment.

6.6 Temporal Resolution

In addition to the spatial, spectral, and radiometric resolution, the concept of temporal resolution is also important in a remote sensing system. The temporal resolution refers to how often the imagery data can be acquired for a specific area (Figs. 6.7 and 6.8). The actual temporal resolution of a sensor depends on a variety of factors, including the platform/sensor capabilities, the swath overlap, the orbit and altitude of the satellite and latitude. Remote sensors in recent satellites have a function to acquire images by tilting to the left and right, and thus the temporal resolution is greatly improved. Most surface-monitoring satellites are in low-Earth orbits (between 650 and 850 km above the surface) that pass close to the Earth's poles. For example, the repeat interval of the individual Landsat satellites is 16 days (Table 6.6). Placing duplicate satellites in offset orbits (as in the SPOT series) is one strategy for reducing the repeat interval. Satellites such as SPOT and IKONOS also have

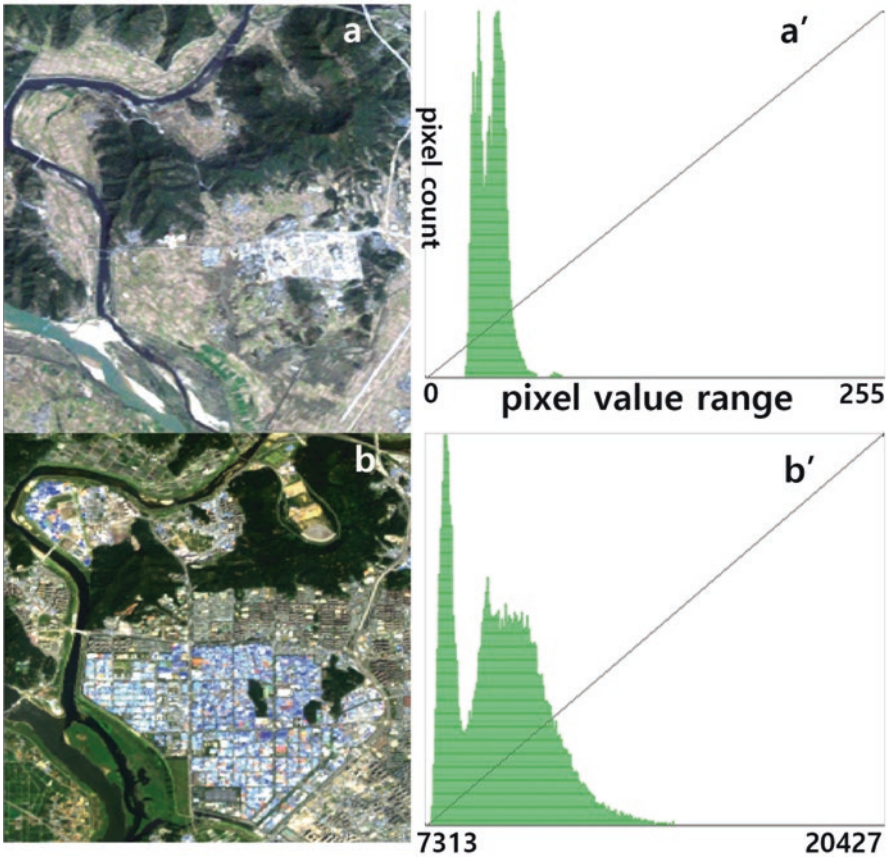

Fig. 6.7 Spatial and spectral variations occurring before and after Sung-su industrial complex construction, Daegu, South Korea, (**a**) October, 1985 (Landsat-5), (**b**) September 2014 (Landsat-8)

sensors that can be pointed off to the side of the orbital track, so they can image the same areas within a few days, well below the orbital repeat interval [10].

The typical satellite has significant limitations in temporal resolution because it acquires an image depending on the sunlight and cannot acquire images properly at night or in bad weather. The actual number of images that can be acquired in a particular area is determined by several variables such as cloud coverage, solar angle, and revisit cycle of the satellite. On the other hand, the satellite using micro wavelength (e.g. ERS-1) emits energy by itself, so the imagery can be collected at all times and temporal resolution is very high.

The surface environment of the Earth is dynamic, with change occurring on time scales ranging from seconds to decades or longer. The seasonal cycle of plant growth that affects both natural ecosystems and crops is an important example. The ability to collect the same area imagery at different periods of time is one of the most important elements for applying remote sensing data. Spectral characteristics

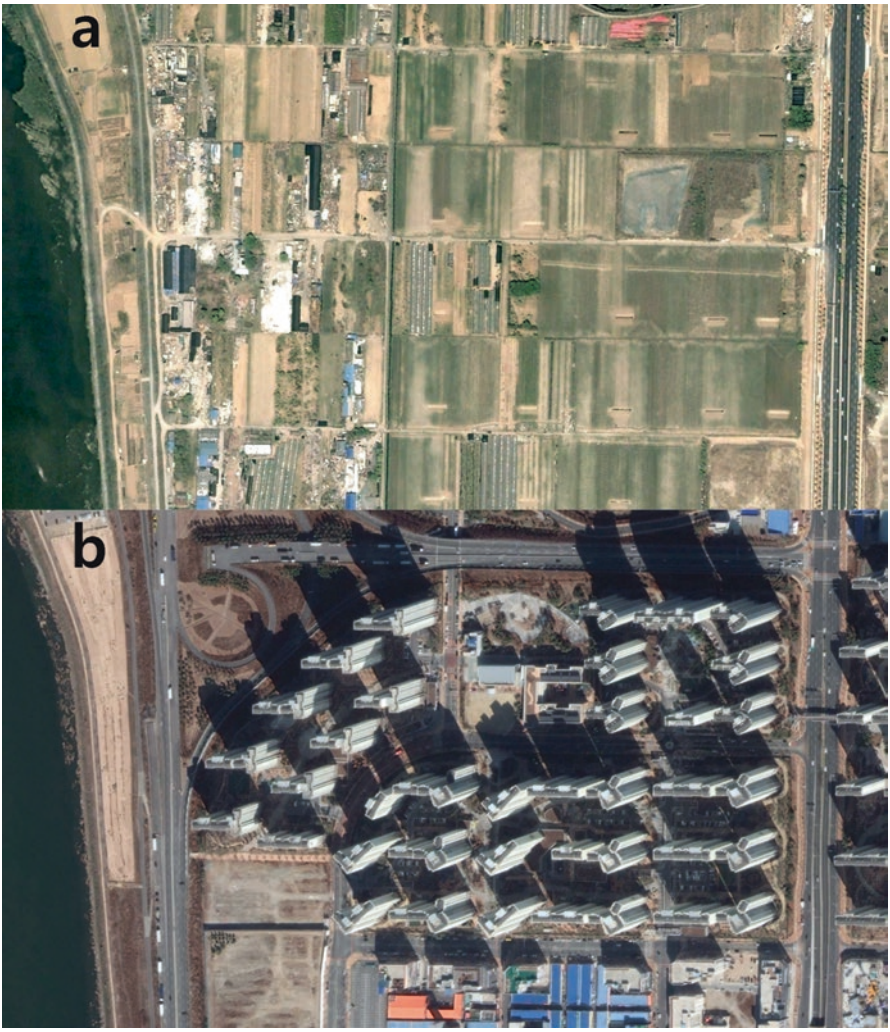

Fig. 6.8 Satellite imagery before and after Isia polis apartment construction (Daegu, South Korea), (**a**) IKONOS (April, 2007), (**b**) IKONOS (February, 2017)

Table 6.6 Temporal resolution of major remote sensing satellites

Sensor	Temporal resolution (days)
Landsat 8	16
GeoEye-1	10
IKONOS	1 ~ 3
Quick Bird	1 ~ 4
IRS	3 (with steering)
	25
SPOT	26

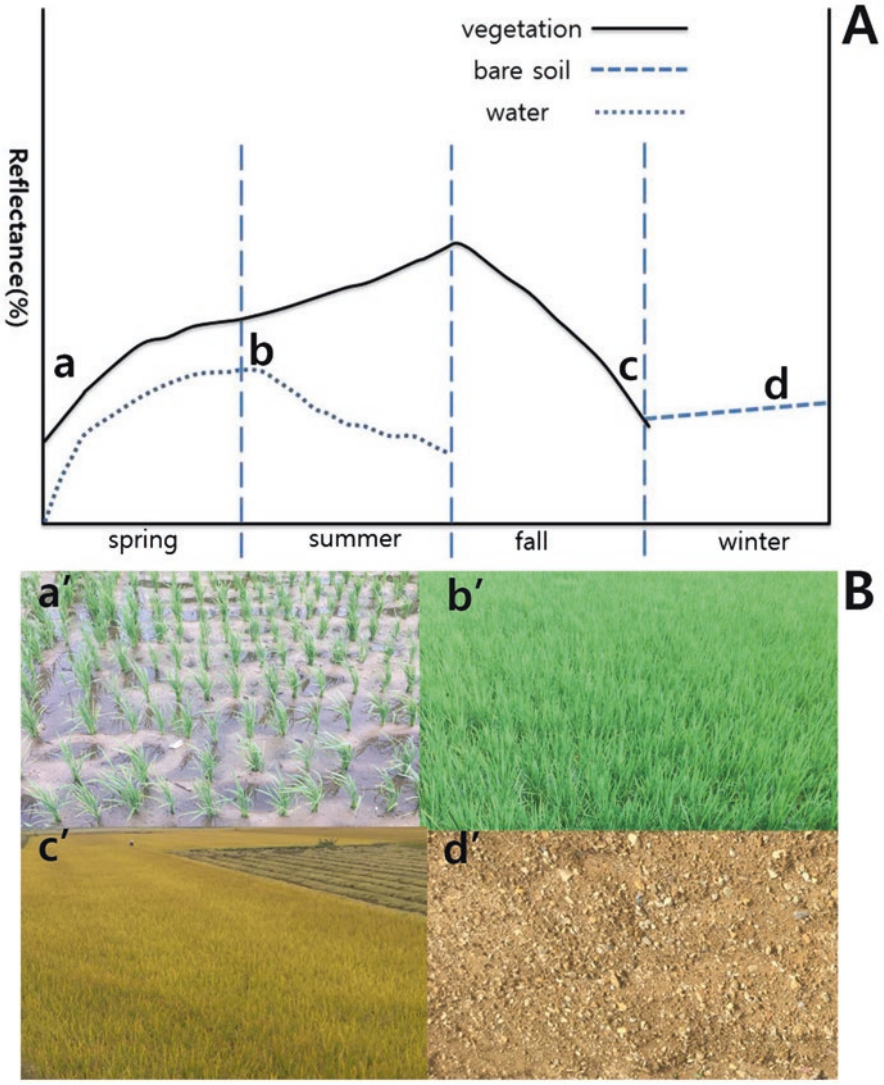

Fig. 6.9 Seasonal spectral response characteristics (near-infrared imagery) of paddy fields and ground photos (South Korea), (**a**) The reflectance characteristics of the ground surfaces (vegetation, soil and water) fluctuating according to the **season**al growth pattern of rice plant in the near infrared imagery, (**B**) Seasonal sequence of ground photos for paddy field, a': spring, b': summer, c': fall, d': winter

of features may change over time and these changes can be detected by collecting and comparing multi-temporal imagery. Thus the image interpretation process can be improved by using remotely sensed imageries taken at different times, whether they are naturally occurring (such as changes in natural vegetation cover or flooding) or induced by humans (such as urban development or deforestation).

Temporal resolution is the most important resolution in applications monitoring the natural environment that changes as often as the weather phenomenon. As the climate is changing in many regions of the earth, the appearance of the ground surface varies with the different seasons. Crops have a unique cultivation cycle, depending on the terrain and climate. Multi-temporal imagery analysis provides information about ground condition changing over time. Information about these changes can be used to identify the process that affects crop growth. Different spectral and spatial variations occurring during the growing season of a crop may not be identified on a single time image (one image on a particular day), but can be identified on multiple date images. Application areas for analyzing rice crop productivity, or calculating the cultivation area of rice paddies will require several seasonal images such as seeding time and harvest time. Figure 6.9 shows the spectral response characteristics (near-infrared images) of vegetation, soil and water in paddy fields. They appear differently season by season according to the growth and cultivation pattern of rice plants. The rice plant showed a distinct difference in the spectral response of near-infrared from the initial transplanting of the rice seedling to harvest. In winter, bare soils of the paddy field mainly affect the spectral characteristics since there is no growing rice. It indicates a strong water response in spring just after transplanting of rice seedling, while the spectral characteristics of typical healthy vegetation is observed in summer when rice is strongly grown. In this regard, the analysis should be appropriately performed according to the season. Analysis using data obtained in different times can easily distinguish paddy fields, showing wetland characteristics in spring and spectral characteristics similar to other crops in autumn.

6.7 Drone Imagery as a Survey Tool for Hyper-Localized Targets[1]

6.7.1 Drone versus Traditional Remote Sensing

Since World War I, aerial photography has evolved in two directions, larger sensor formats for accurate mapping and smaller sensor formats for reconnaissance practice. The former became standardized with large, geometrically precise cameras designed for cartographic measurements (Tables 6.7 and 6.8). The science of photogrammetry was developed for transforming air-photos into accurate maps [11]. Traditional aerial photography using the past film camera is generally collected using a large-format camera (a standard square sensor format, 9″× 9″ film or 230 × 230 mm) mounted on the underside of a fixed-wing aircraft. Photographs were taken sequentially at set intervals, often with a significant amount of overlap

[1]This chapter was revised from author's PhD thesis as shown in the following; J.S. Um, 1997, Evaluating operational potential of video strip mapping in monitoring reinstatement of a pipeline route. University of Aberdeen, Aberdeen, UK

Table 6.7 Comparison of sensor characteristics based on sensor selection criteria

	Landsat imagery	Conventional aerial photography	Drone
Spatial resolution	30 m × 30 m	Better than satellite imagery	Adjustable to user requirement
Spectral resolution	Visible, NIR, Thermal (7 Band)	Visible, NIR, (3 or 4 Band)	Adjustable to user requirement Visible, NIR, Thermal, hyper-spectral
Radiometric resolution (sampling frequency)	usually 8 bit	usually 8 bit	usually 8 bit
Radiometric resolution (imaging condition)	Sensitive to atmospheric scattering, absorption, reflection, etc.	Better than satellite imagery	Better than satellite imagery and manned aerial photograph
Temporal resolution	16 days	About 2 ~ 3 months per year in temperate climate	Better than satellite imagery and aerial photograph

Table 6.8 Remotely sensed imagery utilized in map production.

	Scale	Remotely sensed imagery utilized
Hyper- large scale	Larger than 1/500	Drone imagery
Large scale	Larger than 1/5000	Manned aerial photography
Medium scale	1/10,000–1/100,000	Manned aerial photography/satellite imagery
Small scale	Smaller than 1/100,000	Satellite imagery

(standard end-lap: 60%, side-lap: 30%) to create a stereoscopic view. For digital cameras there is no standard sensor format. The market is divided into large format cameras (as the Intergraph DMC, Leica ADS40 and Vexcel UltraCam), medium format cameras and small format cameras. Most of these cameras have a rectangular image format, where the larger dimension is in the across-flight direction to minimize the number of required flight lines for photo flights. With the advent of digital aerial photography cameras, significantly more vendors are launching products to the market.

It is necessary to understand the difference between traditional analog and digital camera when purchasing a new camera or contracting with a professional aerial photography company [12]. These cameras operate in the same spectral range as conventional analog film including visible and near-infrared, panchromatic, color-infrared, or multiband photography. With the advent of airborne drone imagery in the mid-2010s, another system became available to the environmental manager for remote evaluation of ground targets. With several hundreds of US dollar, the drone can acquire similar or even higher resolution imagery compared to a standard manned aircraft system. Many remote sensing specialists accustomed to interpreting

aerial photography or analysing satellite images now had a 'moving window' to view hyper-local representative sections (building safety inspection, urban stream monitoring etc). UAV photography can provide high spatial details needed by scientists and is not constrained by satellite orbital times or flight schedules of manned fixed-wing aircraft [13]. Various Unmanned Aerial Vehicle (UAV) companies are introducing affordable options for individuals to collect sub-meter aerial imagery directly. These new developments will allow for common access to massive amounts of hyper-spatial resolution imagery at affordable rates over the coming decade. Hyper-spatial resolution imagery introduces the capability of mapping land use and land cover (LULC) of the earth surface with a high level of detail that has led to many new applications.

The flight height of the platform is very different between the satellite and UAV imagery. Thus ground coverage of a single scene is completely different between the satellite and UAV imagery. For this reason, the pre-processing and image interpretation procedure is completely different between the satellite and UAV imagery (Table 6.9). Satellite imagery is processed at various levels ranging from Level 0 to Level 4. Level 0 products are raw data at full instrument resolution. At higher levels, the data are converted into more useful parameters and formats as shown in Table 6.10.

Currently one of the most widely used methods for geometric correction of UAV imagery is based on Structure from-Motion (SfM) algorithms. These algorithms provide the opportunity to create accurate 3D models from image structures without prior information about the location at the time of image acquisition, or about the camera parameters. With the SfM method, the 3D scene geometry and camera motion are reconstructed from a sequence of 2D images which are taken by a camera that moves around the scene. The Sfm algorithm detects common 16 feature

Table 6.9 Comparison of satellite imagery versus UAV imagery

Division		UAV imagery	Satellite imagery
Data characteristics	Flight height of the platform	Adjustable to user requirement	705 km (Landsat 8)
	Ground coverage of single scene	Adjustable to user requirement	170 km × 185 km (Landsat 8)
	Image mosaicking	Necessary	Not necessary
Pre-processing	Data distributed for operational user	Raw data	Pre-processed data at ground receiving station: level 0 to 4 data (NASA)
	Radiometric correction	Not necessary	Necessary
	Ground control	Not always required due to utilizing SfM	Required
Interpretation	Supervised classification	Deep learning (through many layers, hierarchically) still prototype	Shallow machine learning (usually 4–6 multiple layers)
	Visual/manual interpretation	Inadequate (too much time consuming task)	Established as standard

Table 6.10 Data processing levels of Satellite [14]

Data level	Description (NASA-EOSDIS definition)
Level 0	Reconstructed, unprocessed instrument and payload data at full resolution, with any and all communications artifacts (e.g., synchronization frames, communications headers, duplicate data) removed.
Level 1A	Reconstructed, unprocessed instrument data at full resolution, time-referenced, and annotated with ancillary information, including radiometric and geometric calibration coefficients and georeferencing parameters (e.g., platform ephemeris) computed and appended but not applied to Level 0 data.
Level 1B	Level 1A data that have been processed to sensor units (not all instruments have Level 1B source data).
Level 2	Derived geophysical variables at the same resolution and location as Level 1 source data.
Level 3	Variables mapped on uniform space-time grid scales, usually with some completeness and consistency.
Level 4	Model output or results from analyses of lower-level data (e.g., variables derived from multiple measurements).

points in multiple images and uses them to reconstruct the movement of those points throughout the image sequence. With this information the locations of those points can be calculated and visualized as a 3D point cloud [15].

Supervised machine learning has been commonly used for classifying satellite imagery. The shallow or superficial machine learning typically depends on radiometric values of training samples used for classifying the satellite imagery. Hyper-localized target segmentation in super-high resolution images acquired by unmanned aerial vehicles (UAVs) is a challenging task since it requires much more complicated algorithm capable of classifying spatially fine-grained data [16]. Deep learning methods derive their own features (convolution and sub-sampling) directly from the raw data and perform multiple levels of representation for the underlying structure or distribution in the data. Deep learning uses multiple hidden layers and pooling techniques; shallow learning typically only uses one hidden layer according to the user operation having some prior knowledge. The emphasis in shallow learning is on superficial feature detection while in deep learning the emphasis is on defining the most distinctive topology and optimizing hyper-parameters correctly. Automatically classifying hyper-localized UAV imagery with millimeter or centimeter spatial resolution has been dreams of remote sensing experts [17]. It is expected that this dream will come true soon.

6.7.2 Small Sensor Size of Drone Camera

The drawback of conventional small format cameras (36 mm by 24 mm) is that they are still big, bulky, heavy, and fragile when this camera is mounted on the drone. The large sensor size means that each additional payload either increases the size

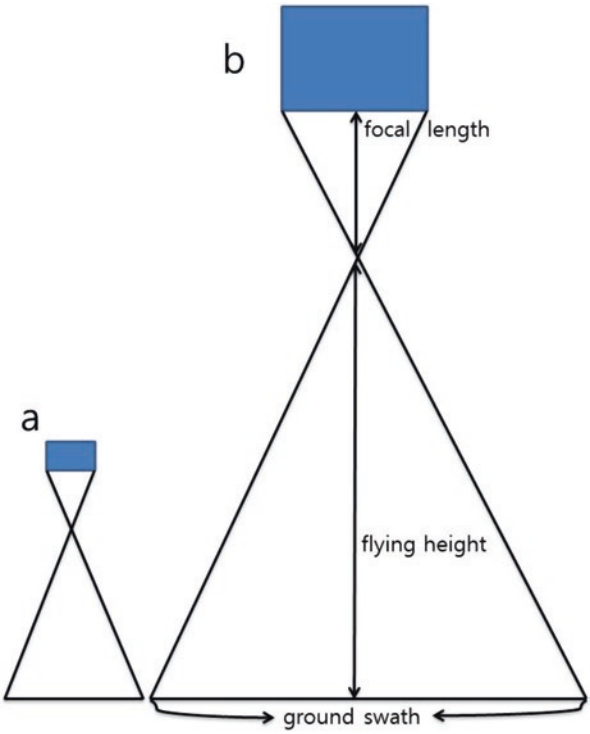

Fig. 6.10 Schematic representation of reciprocal relationship between sensor size and flying height versus ground swath in vertical aerial photograph, (**a**) drone imagery taken with small sensor size at low flight altitude, (**b**) traditional manned aerial photography taken with large sensor size at high flight altitude

and cost of the optics needed or decreases flight time. Most obvious impact of a bigger camera sensor is that it not only will the sensor take up more space in the drone flying part, but it will also need a bigger lens to house an image over it. Stabilizing a larger camera module is also more difficult. With traditional large sensor size (e.g. manned aerial photography), there is much recording of redundant information in hyper-localized target due to wide coverage angle (Fig. 6.10). Traditional large sensors are basically designed for specific wide-area ground targets. They do little to address the monitoring requirements of hyper-localized target in the landscape. Hyper-localized target monitoring represents a potential application for remote sensing which is largely unfulfilled. For drones, larger, heavier cameras also require larger and heavier gimbaling mechanisms. That is why drone manufacturers generally stick with very small sensors. They want to keep devices pocketable and not deal with the bulk of larger lenses.

As sensor technology improves, we're seeing much better performance of smaller sensors [18]. Sensor size is one of the key imaging parameters, along with focal length of the lens, since it is the core component in defining the ground sample dis-

Table 6.11 Examples of small format UAV camera [19]

Camera	Megapixels	Sensor size (mm)	Max focal length (mm)	Compatibility
DJI Zenmuse X3	12.0	6.17 x 4.55	14	Inspire 1
DJI Zenmuse X5	16.0	17.3 x 13	16	Inspire 1
DJI Zenmuse X5S	20.1	13 x 17.3	16	Inspire 2
DJI Zenmuse X4S	20.1	13.2 x 8.8	20.1	Inspire 2
GoPro Hero 4 Silver	12	5.9 x 4.5 mm	30 mm	3D Robotics

tance (GSD: the pixel size in the real world). The small sensor size is an attractive option for those concerned with covering hyper-localized target, or surveying in remote areas, as its light weight can significantly increase flight time (Table 6.11). There are "popular" sensors designed for many compact cameras and phones. Typical compact cameras such as the Canon IXUS 255 HS and the Samsung Galaxy camera use 1/2.3-inch sensors (6.17 x 4.55 mm) [18]. The small sensor size has been the camera of choice for many consumer-level UAV manufacturers (e.g. 3D Robotics, www.3dr.com). Further, the popular DJI Inspire series comes with a built-in camera of very similar specifications to those designed for many compact cameras and phones (DJI Zenmuse X3 of Inspire 1: 6.17 x 4.55 mm sensor size).

The ground sample distance (GSD) is a term to describe the pixel size measured on the ground. For example in an image with 5 cm GSD, a pixel corresponds to 5 cm on the ground. The value depends mainly on the camera sensor resolution, focal length and flying height. The 'ground sample distance' can be improved by reducing ground coverage (by using longer focal length) or by a lower level flight. In drone, improving the ground sample distance is more simple than with other manned airborne sensors, by using the narrow angle-of-view (Fig. 6.10). In fact, to ensure adequate ground coverage for hyper-localized target (e.g. around 10 m width), the sensors with wide-angle of view would require quite heavy optics in terms of focal length and exposure time and a much lower altitude flight specifications than in the case of drone. The reduced ground coverage would also increase the data acquisition cost proportionately for photography. It is not feasible for manned airborne sensors to be used practically for this type of hyper-localized target (e.g. around 10 m width), in terms of flying height, FOV, and cost. Although large format photography has better spatial resolution in terms of absolute value, it is unsuitable for this type of hyper-localized target due to the inappropriateness of the imaging system in terms of wide angle-of-view, cost and low tolerance of image motion [20].

Another important element is the required optimal swath width. Field of View (FOV) differences provided by various remote sensors will find application at different scales. The view-angle of the imaging device must first be carefully considered when trying to obtain remotely sensed data of a long, narrow target. Wide-angle imagery, such as conventional manned aerial photography, generally covers a larger area of land surface than a smaller format system operated at the same altitude and

with the same focal length lens as shown in Fig. 6.10. Any single-scene image collected via such systems covers a wide area of surrounding features in addition to the hyper-localized target. Such an image will, therefore, include a considerable redundancy of information which is not needed for hyper-localized target monitoring. Such wide-area coverage also disturbs the information content of the image by increasing spectral variance, through displaying unnecessary thematic ground classes. This can complicate analysis when doing digital image processing at a later stage [20].

The information content in a remote sensing application depends on the coverage angle of the imaging system if same flight specification (focal length and flying height) is applied. The coverage-angle of the imaging device must first be carefully considered when trying to obtain remotely sensed data of a long, narrow target. Field of View (FOV) differences provided by various remote sensing sensors will find application at different scales [21]. To cover such a narrow swath, the camera should use a zoom lens, which causes some deterioration in photo image quality. Even if it is available, it is not an easy matter to change focal length of a photographic camera while in-flight. On the other hand, a drone camera is almost invariably fitted with a zoom lens operated by remote controller in the ground. In the context of swath/coverage angle, this offers a greater possibility of selecting swath and changing it in-flight if required. This observation demonstrates that drone remote sensing with such narrow angular coverage (requiring a narrow swath) is the system which can be applied in a fairly cost-effective manner to hyper-localized target by covering the necessary ground target precisely.

Aerial drone imagery is a technology that fills a niche that conventional manned aerial photographs cannot meet. Drone remote sensing offers a number of unusual characteristics different from the traditional large format sensors which can be highly advantageous for imaging and monitoring hyper large-scale and hyper-localized target. The characteristics of the ground target are considerably different from the conventional target on which traditional remote sensing has focused. It is necessary to acquire the remotely sensed image from an extremely low altitude, with a narrow angle of view along hyper-localized target [22]. Drone remote sensing can be applied in a fairly cost-effective manner to hyper-localized target monitoring because angular coverage of the camera built in consumer grade drone such as Inspire 1 is much narrower than for conventional photographic cameras.

6.7.3 Low-Height Drone Photography (LHDP)

There are regulations in each country of the world that cover how low an aircraft can lawfully fly. Flying below these heights can be a violation of the regulations, although there are exceptional situations where low flying is permitted.[2] The regula-

[2] These situations include, but are not limited to: flying in the course of taking off, landing or conducting a missed approach, flying in accordance with instructions from an air traffic controller

Table 6.12 Comparison of sensor characteristics for hyper-localized applications

	Satellite imagery	Conventional manned aerial photography	Drone
Cost	Relatively cheap, but, due to limitations in spatial resolution, adequate data cannot be acquired for hyper-localized applications such as building safety inspection.	It is difficult to secure adequate data due to limitations of shooting altitude while the aircraft flight and shooting cost are very expensive.	Hardware purchase cost: Inspire 2 (US$ 4000)
Low-altitude tolerance	No	No	Yes
User friendliness	Intermediate	No	Yes
Image motion tolerability	Yes	No	Yes

tions usually require that pilots fly no lower than 300 m (1000 feet) over built-up areas, or 150 m (500 feet) over any other area (rural area). For instance, Federal Aviation Administration (FAA) is the government agency responsible for aviation safety in United States and its territories. According to the Code of Federal Regulations in the USA (Section 91.119 of the General Operating and Flight Rules), a manned aircraft would not be allowed to fly lower than 150 m (500 feet) over other than congested areas and not less than 300 m (1000 feet) over congested areas of a city, town, or settlement.[3]

In order to monitor hyper-localized target (e.g. urban stream with around 10 m width), it is necessary to acquire the remotely sensed image from an extremely low altitude, with a narrow angle of coverage. This means that low-level flight with small photographic format violates the regulation. Low-level flight also causes serious image motion and it should be compensated with a faster shutter speed in very bright conditions. Over the last 20 years or so, the majority of remote sensing has been used to support global, national, or large area applications. As a consequence, those charged with more target specific requirements, such as the building safety inspection, have benefited far less from the fruits of that conventional research. The high cost of photo acquisition, particularly for a scattered hyper-localized target, is a significant disadvantage of the manned photographic survey method. With drone remote sensing, the scattered hyper-localized target may be recorded all on the same day. Additionally, drone remote sensing is much less expensive than most other remote sensing systems (Table 6.12). Due to such low-cost data acquisition, this

undertaking certain kinds of specialised aerial work, for example, power line inspection, geographical survey work, aerial firefighting, agricultural spraying.

[3] 91.119 – Minimum safe altitudes: General. [Doc. No. 18334, 54 FR 34294, Aug. 18, 1989, as amended by Amdt. 91-311, 75 FR 5223, Feb. 1, 2010] Except when necessary for takeoff or landing, no person may operate an aircraft such altitudes. A helicopter may be operated at less than the minimums over congested areas and other than congested areas, provided each person operating the helicopter complies with any routes or altitudes specifically prescribed for helicopters by FAA

technology may have a particular value in highly changeable areas, such as rooftop temperature and the monitoring agricultural crop harvests, where year-to-year, day to day, hourly and seasonal changes are common. Large-scale changes for various ground targets could be monitored, thus, monthly or seasonal survey results could be updated on a site-specific basis.

Airborne drone monitoring programs, aided by the use of conventional sampling, can complement the present field survey in an optimal way. This method will provide information efficiently, that is both scientifically justifiable and practically understandable by the customer [23]. The high cost of aerial photo acquisition, particularly for a scattered target such as an urban stream with around 10 m width is a significant disadvantage of the conventional manned photographic survey method. With airborne drone survey, the long linear extent of corridor targets such as the urban stream could be recorded all on the same day. The time and cost of post-processing are virtually eliminated by providing instantaneous real-time imagery, much more quickly than with the field survey. It is much less expensive than in-situ survey systems [24].

Monitoring is fundamental to any development projects both to assess adherence to national regulation and to support management options. Monitoring can be considered at a pre- or post-decision project stage. Pre-monitoring, called baseline monitoring, measures the initial state prior to implementation of a proposal. Post-decision monitoring includes monitoring activities undertaken to determine the impacts or changes to the environment caused by the proposal once it has been implemented (environmental effects monitoring) [25–27]. Environmental monitoring to communicate information about the environment and human activities is emerging as a global trend and applicable to all types of organization (e.g. government or private companies). It equally covers activities undertaken to ensure that environmental components are not altered by human activity beyond a specific standard or regulation level (compliance monitoring) [27].

Especially in development projects requiring the EIA (Environmental Impact Assessment), impacts of projects need to be monitored on a regular basis during the entire project life cycle. The comprehensive EIA is accomplished by gathering information about socio-economic, biological and physical setting, to evaluate potential interactions between the environment and the activities associated with development projects. Developers are obliged to monitor the significant environmental effects of the implementation of plans and programs in order, inter alia, to identify at an early stage unforeseen adverse effects, and to be able to undertake appropriate remedial action. This baseline assessment establishes the current environmental conditions of the site and its surroundings. The environmental inventory is intended to describe the condition of the site on which the project is to be built as well as its environmental characteristics, including key ecological interactions, sufficiently precise, clear and transparent to enable individuals to ascertain their rights and obligations.

Utilizing area-wide spatial information in the EIA process is one of priority issues to assure and improve public communication and participation. The main intentions introducing drone imagery is to communicate information about the environment

and human activities. The drone image can be especially useful to highlight emerging significant environmental impacts during monitoring programs. Further drone imagery could provide evidential information for EIA performance, such as regulatory compliance, mitigation performance, validation of impact-prediction and verification of residual effects [25]. Drone imagery could be used to verify predicted impacts and confirming the effectiveness of mitigation measures (e.g., auditing of compliance with environmental legislation and with site specific environmental protection plans) since it is presented as a permanent record at the various timing of construction (pre-construction, during construction, or post-construction as applicable).

The funding and number of personnel that were available to do ground monitoring 10 years ago are now generally unaffordable, while the cost of drone remote sensing data is getting much cheaper, and it is more powerful in terms of information content than before. The collection of field data via drone remote sensing is, therefore, proposed as a practical, cost-effective alternative. Drone imagery provides a permanent visual record for the pre-construction and post-construction phases of any project (e.g. building, bridge, road etc). It is particularly useful for assessing a variety of spatial and temporal characteristics of various development activities [23].

6.7.4 Low-Height Drone Photography as an Alternative for In-situ Survey

Fundamental advantage of using UAVs is that they are not burdened with the physiological limitations and economic expenses of human pilots. Most of the UAV systems on the market are less expensive and have lower operating costs than manned aircrafts. UAVs are increasingly seen as an attractive low-cost alternative or a supplement to in-situ terrestrial photogrammetry due to their low cost, flexibility, availability and readiness for duty [28]. In addition, UAVs can be operated in hazardous or temporarily inaccessible locations. Major advantages of LHDP (low-height drone photography) compared to manned aircraft systems are that UAVs can be used in high risk situations without endangering a human life and inaccessible areas, at low altitude and at flight profiles close to the objects where manned systems cannot be flown. These regions are for example, natural disaster sites, e.g. mountainous and volcanic areas, flood plains, earthquake and desert areas and scenes of accidents. In areas where access is difficult and where no manned aircraft is available or even no flight permission is given, LHDPs are sometimes the only practical alternative [28]. They also, if properly used, increase the safety of people conducting measurements, because an operator can stay out of a dangerous zone.

The "primary advantage of LHDP is the ability to bridge the scale gap between field-based observations and manned airborne or satellite observations. For low-height applications, it was usual that in-situ terrestrial survey has to be implemented

Table 6.13 Comparison of UAV imagery versus field survey point photo

	UAV remote sensing	In-situ survey
Data acquisition area	Area-wide information in a short time	Fragmented information only for survey sites
Objectivity of information	There is little controversy involving the subjectivity of the investigator since the remote sensing data is presented as permanent record.	Since the position of the investigator changes from time to time, subjectivity may be involved depending on the sample location.
Accessibility of survey points	There is no obstacle because it is approached through low-altitude flight considering spatial variables over survey point	There is always a restriction to accessibility, due to safety and time-consuming task such as water-body and mountains.
Position accuracy	The position of the real world is accurately displayed because it is collected at the vertical vantage point available at map and ortho-photo.	It is performed from horizontal perspective, so it has considerable limitations in matching the survey results to real world position in terms of map coordinates.
Expenses	Cheap	Expensive
Change detection	It is easy to acquire data in a timely when an investigator needs to acquire data.	The results presented by tables and figures have significant limitations in performing change-detection because it is impossible to quantitatively analyze the various variables such as the natural environment and human environment.

as alternative arrangement (Table 6.13) since remote sensing projects are quite often not feasible due to the expenses for manned aircrafts. LHDP can be seen as supplement or replacement to terrestrial in-situ survey in many fields of applications. In the case of combination of terrestrial in-situ survey and UAV photogrammetry, it is even possible to use the same camera system and having the same distance to the object, which simplifies the combined data processing [28]. With the advent of hyper-spatial resolution imagery of drones, many objects and shapes that have not been seen in satellite images and manned aerial photograph have become apparent. The images taken by the drone can identify people or road lanes that have not been distinguished from high resolution satellite images or aerial photographs. As the spatial resolution of the image is improved, the identification range of the object is also widened. Remote sensing applications have focused on more than medium scale environments such as ocean, atmosphere, forest, and water resources.

However, the emergence of drones has expanded the scope of remote sensing, which requires detailed information such as building inspection, power-line monitoring and individual tree analysis. It is now possible to observe urban facilities, such as buildings and traffic facilities, that can be identified at a high resolution of less than 10 cm. LHDP shorten the time of performing surveys (from several days

to few hours) that have to be spent in a field. New products such as colorful overview maps and detailed CAD models of buildings can be delivered to the customer just after drone flight. Much of the data acquired by current field surveys is expected to be replaced or complemented by unmanned aerial imagery that allows intensive investigation of specific locations [29]. Furthermore, much of the remote sensing area that used manned aircraft images or high-resolution satellite imagery in the past is likely to be replaced by drones.

6.7.5 Decreasing Cost of Hyper or Multi-spectral Sensors

Visible wavelength sensor (e.g., RGB sensor) usually only provide information on a very limited number of bands and/or spectral ranges. It might not work for very detailed land mosaic components that characterize hyper-localized targets, such as a solar-powered house rooftop or a building safety inspection target. To tackle this issue, hyper-spectral sensors, commonly used on satellites or manned aircraft a few years ago are getting redesigned to be lighter and smaller. Thus, UAV is now more suitable to bring the sensor with a wider spectral range and narrower bands [29, 30].

New sensors with multi-spectral sensitivity are rapidly emerging into UAV platform, making high-resolution infrared sensors not only smaller and more lightweight, but also less expensive (Fig. 6.11). Decreasing costs for sophisticated infrared sensors makes UAV platform accessible from a growing number of innovative new applications. Hyper-spectral sensors also are decreasing in size, weight, and cost to increase the availability of these technologies [31]. UAV carrying advanced hyper or multi-spectral sensor proliferate in various applications, in the air, on the ground and at sea [32, 33].

Thermal infrared sensing is becoming far more sophisticated today than simply detecting warm objects. This approach continues to detect and classify humans and animals from the warmth of their skin, as well as land vehicles, aircraft, and industrial sites from their hot engine exhaust. Further blending visible sensors with thermal infrared can detect humans, animals, and vehicles quickly against a cool background [31, 34]. Hyperspectral sensors usually generate huge amounts of data since they retrieve spectra sets composed of hundreds of bands across considerable spatial resolution images. It is expected that the technological development of upcoming years can bring smaller and more affordable devices, turning hyperspectral-based sensing into a mainstream approach for agriculture, forestry and related areas [30].

Satellite and aerial imaging are generally referred to as passive, because they measure radiation from an external source (i.e. sunlight). LiDAR (light detection and ranging) and RADAR (Radio Detection and Ranging) are considered active, as they are not dependent on sunlight, but rather emit their own radiation. LiDAR uses a laser to produce and emit pulses of light, and measures the time it takes for a reflection of this pulse to return. LiDAR is a remote sensing method that uses a laser to measure distances. When learning about LiDAR, one is likely to encounter terms

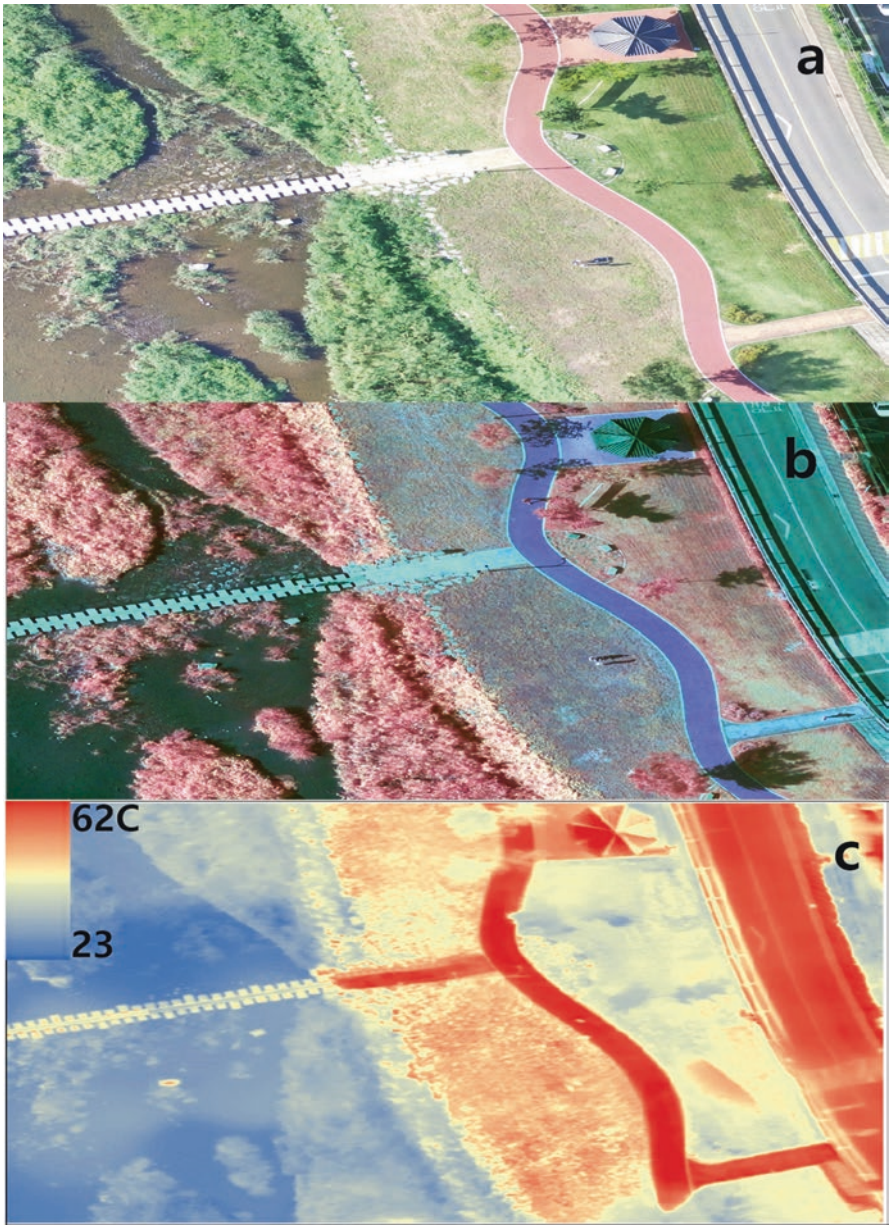

Fig. 6.11 Example of multi-spectral imagery taken at UAV platform, (**a**) visible imagery, (**b**) near-infrared imagery, (**c**) thermal infrared imagery

like airborne or terrestrial LiDAR, or aerial or terrestrial laser scanning. A LiDAR device itself can be mounted on an airplane, helicopter, drone, car or tripod. In the typical case, the LiDAR device is mounted on board an airplane and the system

scans [35]. At present, extremely compact laser scanners became commercially available. UAV-based laser scanning (ULS) is a new segment complementing the existing applications for lidar technology, such as airborne, mobile, and terrestrial laser scanning. UAV-based laser scanning (ULS) provides extremely flexible and cost effective operation possibilities, delivering comprehensive and accurate data in combination with ease of operation and low cost [36]. It shows high potential for various applications.

The laser emits millions of such pulses of light and when the pulse hits a target, signals representing the target are reflected back to the laser scanner. They record a highly precise 3D-point cloud which can be used to estimate the 3D structure of the target area (digital elevation model). This technology provides real-time and autonomous 3D-point clouds data on the fly and ground. LiDAR provides the most accurate data on 3D structure of any remote sensing technique [35]. The performance of UAV-based laser scanning has shown remarkable results during the last decade, including ground surface scanning at night, electrical powerline, carbon storage and vegetation roughness scanning as well as texture scanning of various ground objects (e.g. bridges, buildings, daylight mining area, etc.) [37]. Future LiDAR datasets will likely include multispectral properties and improved spatial and temporal coverage and resolutions. REDD+ (Reducing Emissions from Deforestation and Degradation) is a UN framework designed to support financially as an incentive for the protection of carbon contained in forests. LiDAR has been increasingly used for mapping above-ground forest biomass and for estimating forest carbon stock, since it has capability to penetrate the forest canopy and determine the three-dimensional structure of the target [38].

6.7.6 Sunrise Calendar Temporal Resolution

Change-detection' means to identify and locate changes in imagery of the same geographic area obtained at different times. The information is extracted by comparing two or more images of an area that were acquired on separate occasions. This approach is frequently taken to monitor area-wide Earth features by satellite remote sensing (such as deforestation monitoring, detection of crop-yield change and land-use changes, such as urban fringe change due to urban development). Traditionally, such change-detection has been conducted by manual interpretation of aerial photography. A problem associated with using historical remotely sensed data for change-detection is that the data are usually of non-anniversary dates, with variations in sun angle and in atmospheric and ground moisture conditions.

A key advantage of unmanned platforms in change detection is a constant availability. Manned missions can be limited by human endurance factors, whereas unmanned aerial vehicles (UAVs) can survey the area of interest for 24 h or more (Fig. 6.12). The change-detection study assumes that the multi-temporal imageries have been collected under similar conditions (e.g., the camera is pointing vertically downward and lens distortion has a negligible effect). The effect of atmospheric

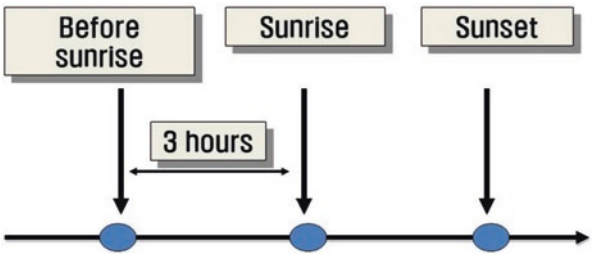

Fig. 6.12 Schematic representation of theoretical principle involved in sunrise and sunset calendar temporal resolution

turbulence or other distortions in the images should be negligible. It is also assumed that changes in plant condition are accompanied by corresponding changes in leaf reflectance characteristics. However, any study dealing with several images should also consider the problems of image combination. Elements such as geometric position, atmospheric effects, or radiometric equivalence are very difficult to correlate in several images [39].

In a temperate region such as the UK, South Korea, there are only a few months in the year with the necessary bright light conditions for manned aerial photography. On the whole, the reduced illumination conditions of winter do not favor manned aerial photography. Such weather conditions do not allow the data acquisition with large format cameras integrated into manned aircrafts due to required high flight altitude above ground. However, in cloudy and drizzly weather conditions, the data acquisition with LHDPs is still possible, when the distance to the object permits flying below the clouds [24]. LHDP have particular advantages in terms of temporal resolution. Because the user has a platform, it has the advantage of being able to shoot at any place at any time. It can be dispatched to a disaster site (for example, a fire) that occurs without notice, and a necessary image can be collected. It is particularly advantageous in applications that monitor changing site conditions through day by day, the seasons or during a period of years repeatedly such as traffic congestion and agricultural crop analysis [28].

Even with a wider angle of view, it is difficult to ensure coverage of the hyper-localized target using manned aerial photography from low altitude. It is difficult to send aircraft frequently to the survey area since manned aerial photographs are expensive to shoot. Target navigation problems can be much less troublesome with drone since it is possible to review an image strip in real-time and correct for any gaps in coverage by flying the drones again. Moreover, great advantages of drone imagery in change detection are the real-time capability for fast imagery acquisition, while transmitting the geo-referencing and orientation data (GPS, INS etc) in real time to the ground control station (Fig. 6.13). For hyper-localized target such as house, road and urban stream, it is necessary to fly at very low altitude with longer focal length to achieve a narrow ground swath. This specification requires the use of very fast shutter speeds, such as 1/2000s, to avoid image motion. For example, with the popular drone camera sensor size of 6.4 mm by 4.8 mm, it is possible to cover a 40 m swath from 100 m flying height, without any difficulties in terms of image motion and flight regulation. As a result, the use of airborne drone data would fill an

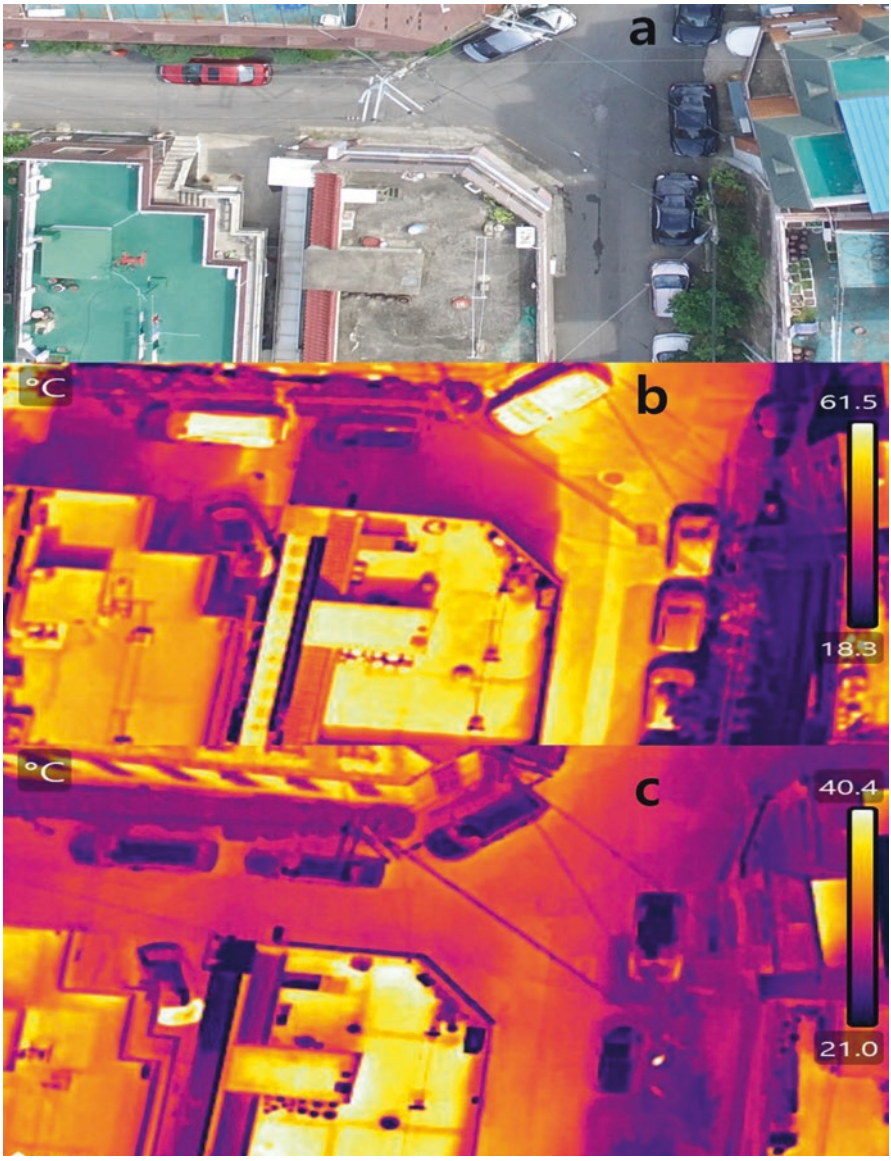

Fig. 6.13 Thermal-infrared imageries taken before and after sunset. (**a**) visible imagery (**b**) thermal imagery taken at 15:00 PM Sept 3, 2017 (**c**) thermal imagery taken at 20:00 PM Sept 3, 2017

existing gap with its ability to detect change of hyper-localized target quickly and under conditions of weather and time that would render manned aerial photography inadvisable. This is a very important attribute of drone imagery for low-level change detection application [20].

Radiometric equivalence is another source of problems in change-detection studies, which arises from differences in illumination conditions among multi-temporal images. Because the mechanism of acquiring remote sensing imagery varies so widely with the systems used, direct comparison of imagery acquired with different systems at different dates can be quite difficult. Radiometric calibration involves direct comparison of the brightness with the amount of radiance received by the sensors, which depends on several complex factors. It is very difficult to calibrate the grey value difference since related environmental factors at the time of image acquisition are too dynamic to control. Without radiometric calibration, it would be difficult to quantify and interpret change in multi-temporal images since there would be no clear baseline to compare spectral reflectance differences between the same ground objects. In particular, remote sensing has been avoided for multitemporal applications because of radiometric calibration problems, real or perceived.

Atmosphere will affect EMR (Electromagnetic Radiation) in three ways (absorption, transmission and scattering). Atmospheric distortion can occur anywhere in information flow (Sun → Surface → Sensor). Atmospheric conditions weaken the intensity of sunlight incident on the sensor and consequently affect the radiometric fidelity of the imagery. Manned aerial photographs are significantly exposed to distortion due to the atmosphere. This is because sensors located at an altitude of 300 m or more are affected by various atmospheric conditions such as clouds and dust in the process of detecting electromagnetic waves reflected from the ground surface. There are many problems in ensuring radiometric fidelity so that change detection can be performed if the weather conditions are not exceptionally clear since the manned aircraft has a fundamental limitation in lowering the shooting altitude. In the case of drones, the distance between the sensor and the ground object is much closer to that of an aerial photograph, and it can take close-up pictures, so it is less affected by the atmosphere. Therefore, it is considered that the drone image guarantees better radiometric fidelity than other remote sensors. Therefore, the high radiometric fidelity means that radiometric equivalence for the change detection is high. UAVs have the advantage of flying closer to the earth surface wherein the influence of the atmosphere is not as significant. For this reason, there is no need for atmospheric corrections as it would be in traditional platforms [30]. Thus, drone imagery has frequently been analyzed to compare relative spectral differences between features with special attention to the absolute radiance or reflectance differences being imaged [40–44].

6.8 Drone Shooting and Related Observation

In designing a drone flight system, many options of sensors (such as no GPS, GPS and DGPS) affect the quality of the data that can be acquired. A successful UAV flight is one where sensors are properly used to accomplish tasks. UAV platforms can be classified according to their integrated location sensors and real-time imaging capability, which influence directly the autonomous flight performance.

High-end sensors, such as DGPS and navigation-grade IMU (Inertial Measurement Unit) have the potential for real-time geo-referencing while low-cost sensors will imply post geo-referencing. Nowadays, the autonomous flight based on defined points in a global coordinate system is a standard approach to collect the nadir drone imagery (Table 6.14). Autonomously flying UAVs provides the overlapped imagery for further photogrammetric processing. However, prior to a successful UAV operation, an extensive mission planning is necessary. This mission planning is dependent on the kind of application and in particular on the specific situation at the flight area. The autonomous flights still have to be performed with a backup pilot in line of sight (LOS) due to security of people and obstacle avoidance in certain emergency situations [28].

The aerial photographs taken by UAV platforms can be classified according to the orientation of the camera axis. The oblique imageries were usually acquired by common UAV users, while traditional nadir images were collected in a number of mapping applications. True vertical photograph is a photograph with the camera axis perfectly vertical and such photographs hardly exist in reality. The near vertical photograph is a photograph with the camera axis nearly vertical. The deviation from the vertical is called a tilt that is usually less than two to three degrees. Gyroscopically controlled mounts provide stability of the camera so that the tilt must not exceed platform-driven tolerance for further photogrammetric processing. The UAV platform operated by rotary wing allows vertical take-off and landing without the need for an available runway. Furthermore, the use of VTOL (vertical take-off and landing) systems permits the image acquisition on a hovering point, while the camera is turning in the vertical and horizontal direction [45]. For the oblique imagery control is mostly done in the manual or assisted flight mode. The oblique photograph is a photograph with the camera axis intentionally tilted between the vertical and horizontal. A high oblique photograph is tilted so much that the horizon is visible on the photograph. A low oblique does not show the horizon. The total area photographed with oblique is much larger than that of vertical photographs. 3D reconstruction for any target can be performed by drone imagery since oblique images can allow the observation of vertical structures (e.g., including transmission line and building footprints) [46–48].

Table 6.14 Example of flight log file (DJI Inspire 1)

Longitude	Latitude	Height (GPS)	Height (barometer)	Number of GPS satellites
128.7264	35.8443	47.0316	49.702	16
128.7264	35.8443	47.2684	49.7039	16
128.7264	35.8443	46.6589	49.7037	16
128.7264	35.8443	47.0159	49.7009	16
128.7264	35.8443	46.523	49.7011	16
128.7264	35.8443	46.4545	49.6984	16
128.7264	35.8443	46.5125	49.699	16
128.7264	35.8443	46.4744	49.7017	16
128.7264	35.8443	46.9396	49.7026	16

The autonomous flight is most suitable for photogrammetric data acquisition, since the planned flight route can be flown without manual operation by ground pilots. The autonomous flight capability for the application requirements can vary among the large spectrum of flight planning software and existing UAVs. The commercial mission planning packages (for instance, Pix4D Capture) usually have a function combining the classical flight planning applied in large-format aerial photography and the close range terrestrial photogrammetry. The software controls UAV while it is flying and collecting images so that the mission can be fully automated, but it is also possible to take over manual control in case of emergency situations (Fig. 6.14). With the commercial mission planning packages, it is possible to choose a mission among several parameters. It allows you to create flight plans for capturing image data and set up the main project parameters like appropriate overlap percentages, flight altitude or flight speed, the flying mode, coordinate system and camera parameters (e.g. viewing angle), the definition of the photographing target area in a graphical interface (Fig. 6.15). The photographing target area can be defined by describing the boundary in a map using a GIS system, as well as in a 3D world viewer like Google Earth, Virtual Earth etc.

The predefined flight path can be exported to Google Earth in the KML data format. This procedure allows one to check the flight path to cause possible collisions in the local environment such as super-high rise building and electric powerline. Pix4D Capture supports flexible flight mission (grid, double grid, polygonal,

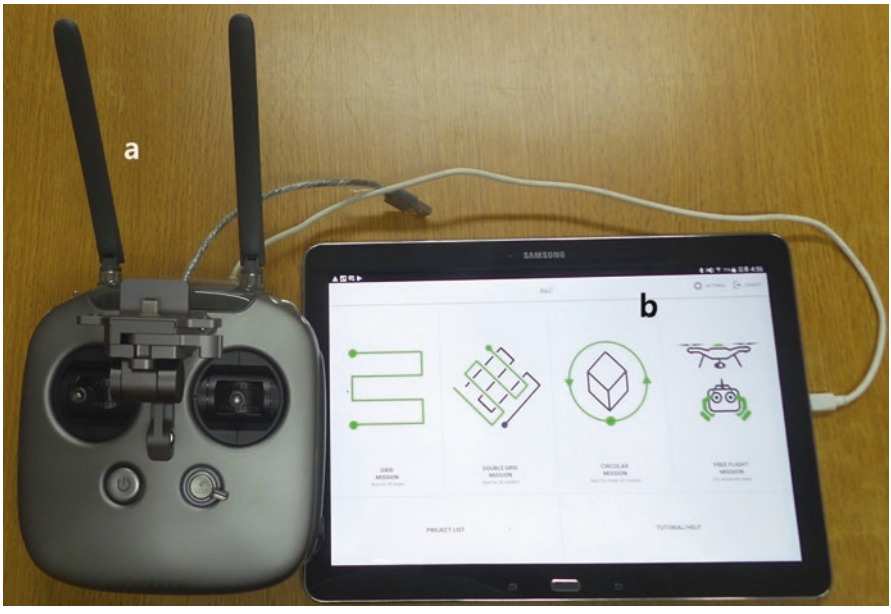

Fig. 6.14 User-interface for flight missions in the commercial UAV mission planning package, (**a**) remote controller, (**b**) flight missions (grid, double grid, polygonal, circular mission) available in Pix4D Capture

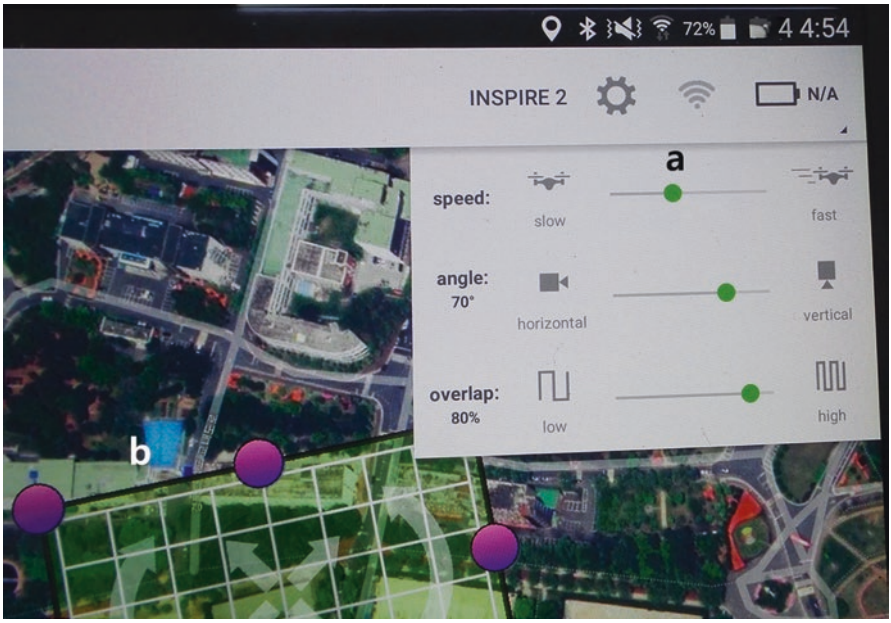

Fig. 6.15 User-interface to select flight parameters in Pix4D Capture, (**a**) Main project parameters (overlap percentage, flight speed, and camera viewing angle), (**b**) predefined flight path overlaid to Google Earth

circular mission) to accommodate diverse project requirements. There is a polygon mission to plan a project over an arbitrary and irregular area. Grid mission allows the drone to perform a flight over a rectangular field while a Double Grid mission to also fly over a rectangle but in both directions (Fig. 6.16).

The photogrammetric block is based on one or more areas of interest defined interactively by the user and consists of an origin point (start point or take-off point), a final point (home point or landing point), and an initial block direction together with the accomplishment of certain photogrammetric constraints. Strong wind disturbs UAV in realizing a perfect, preplanned flight projects. Strong wind disturbs UAV in navigating a pre-planned flight routes in autonomous navigation. In particular, in the case of a light-weight UAV (DJI Inspire 1: 2935 g), the wind causes a profound effect to stable flight. If the UAV were flying at 10 m/s speed, and the wind speed in opposition direction was 10 m/s at that time, then principally the UAV could not go to its own destination and only consumes the battery. Such instable flight will cause holes in imagery overlap and seriously influence the quality of the produced ortho-photos since it does not follow pre-defined flight route for autonomous navigation.

Temperature is the most important factor in the normal operation of a UAV-loaded battery. The flight time of the UAVs depends on battery performance, since propulsion devices such as motors and propellers are driven by the energy powered from battery. Almost all UAVs use a lithium-polymer battery (e.g. DJI Inspire 1).

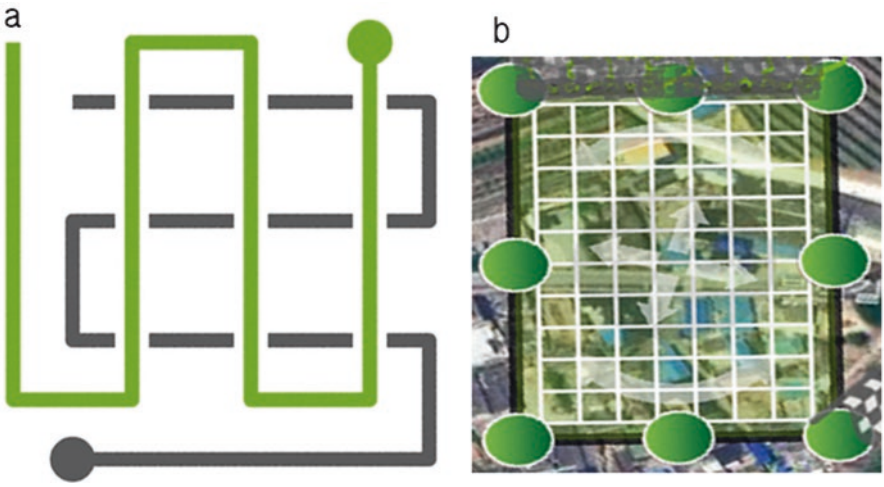

Fig. 6.16 User-interface showing Double Grid mission and a rectangular boundary (Pix4D Capture), (**a**) Double Grid mission to fly in both directions, (**b**) rectangular boundary overlaid to Google Earth

Basically, batteries produce energy through chemical reactions. But they do not react well at above or below the proper temperature range. Batteries will lose much of their capacity when exposed to cold temperature since it adversely affects chemical reactions of battery until the batteries warm up. In below 0 °C weather, the electrons slow down and the battery voltage does not come out properly. Inspire 1 User Manual indicates that the performance of the intelligent Flight Battery is significantly reduced when flying in low temperature environment (those with air temperature below 5 °C) [49].

The sunlight affects the quality of the images that are taken and too bright or dark lightning. If it is sunny, objects in the photos will be well visible but there also will be shadows. On the other hand, when the sun is not shining and it is cloudy, the terrain is uniformly exposed but also dark. A compromise between two approaches must be made to capture appropriate images. Good lighting will reduce grain, and will result in having a high shutter speed which reduces motion blur. Visual aspect of final photogrammetry products can lead to difficulties for software (such as Pix4D mapper or photoscan) to do post-processing aligning the photos.

6.9 Ortho-Photo Generation

6.9.1 Bundle Block Adjustment

A single aerial photograph presents a picture of a portion of the earth's surface. Because the single aerial photograph is limited in an area, groups of photographs are combined into mosaics to provide the area-wide pictorial view of ground

coverage. However, certainly to achieve the area-wide visualization, human labor and cost required in the time-consuming mosaicking process would be the serious constraint [50]. A stereopair of the aerial photograph consists of two photos of the same object that allows it to appear in three dimensions by photogrammetric processing. The imagery is commonly collected with a 60% overlap in the flight direction (forward overlap) and 30% to the sides (sidelap) across a flight path with a wide angle lens.

Photogrammetry is the art and a science of performing accurate measurements from 3D photographs generated using overlapped 2D images. It is a tool to generate spatial and descriptive information reconstructing objects by utilizing data acquired from remote-sensor without touching targets. The output of photogrammetry is ortho-photo represented in their true positions in relation to their ground position. There are two general types of photogrammetry; aerial photogrammetry and close-range terrestrial photogrammetry. Ortho-rectification is the process of removing the image distortion induced by the sensor taking perspective view, and relief displacement for the purpose of creating a geometrically correct image. Ortho-photos can therefore be used to make direct measurements of distances, angles, positions, and areas without making additional geometric corrections for relief displacements. As imageries taken from UAV are widely available, the digital ortho-photo has become a very common part of spatial datasets. In order to generate the ortho-photo, various parameters for terrain are needed and they can be derived using either a bundle adjustment using photogrammetry or by fitting the image over some known ground control points (GCP). GCP is a point with known coordinates, that is located in the area of interest and recognizable in the photos. The location of any point in an image is labeled with two coordinates (x, y) since images are only two-dimensional. The location of any point in the real world is defined by three coordinates (x, y, z, latitude, longitude, altitude) since the real world is primarily three-dimensional. 3D models can be generated from either nadir imagery (shot vertically, straight down) or oblique imagery (from an angle to the side), but the most detailed models combine both into a single representation [51]. Overlapping images taken from a different location allow us to determine the 3D location of the point.

This process requires the position and orientation of the camera during the exposure. Bundle Block[4] Adjustment (Fig. 6.17) is a method to directly compute the relations between image coordinates and object coordinates and is a basic tool in the photogrammetric data handling. It is time consuming procedures to determine the photo orientation individually for each photo or model based on control points. All images of a block are connected together using corresponding points, "gluing" them to a mosaic which is then transformed to the GCPs [52]. It is common to place a set of reference markers with known 3D coordinates during collecting camera positions and identify them manually in the images. The photogrammetric block is based on one or more areas of interest defined interactively by the user and consists of an origin point, a final point, and an initial block direction together with the camera orientation parameters. Block adjustment not only links image coordinates with the

[4] All images covering an area and being processed in a block adjustment.

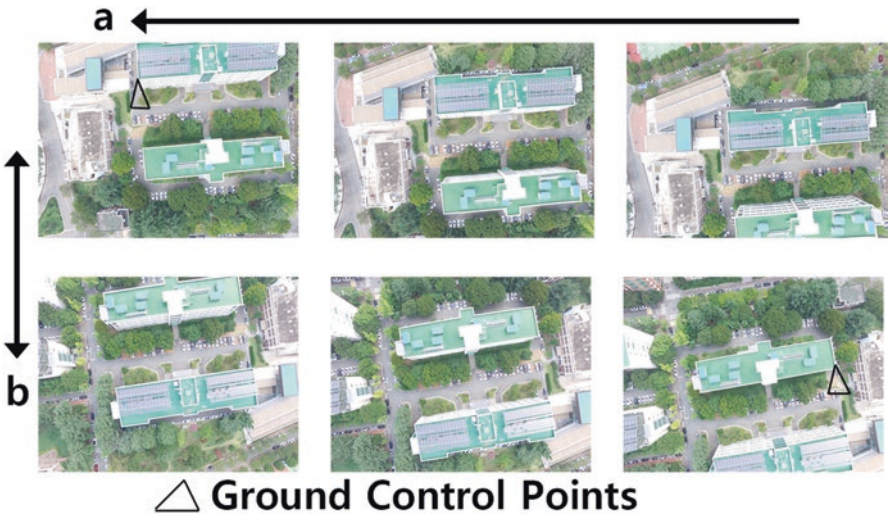

Fig. 6.17 Concept of bundle block adjustment, (**a**) end-lap (overlap between neighboring images), (**b**) side-lap (overlap between neighboring strips) Adding another image taken from a different location allows us to intersect the rays and determine the 3D location of the point where the light came from

real world location, but also connects between overlap images of a mosaic dataset. Bundle block adjustment reduces the cost of field surveying and verifies the accuracy of field observations during the adjustment process [53].

Once, the coordinates acquired by indirect (GCP) or direct (GNSS) geo-referencing are obtained, they can be processed in a bundle block adjustment. This geo-referencing can generally be done indirectly using ground control points, or directly using an on-board sensor system. The indirect geo-referencing can be performed by conventional methods, i.e. total station survey to calculate coordinates for known ground points (Northings, Eastings, and Elevations) and GNSS or acquired from other available sources, like internet map service or old maps. Since an indirect geo-referencing is very time consuming, and also not available in real time, many users would prefer a direct geo-referencing. GNSS measurements in indirect geo-referencing are the most efficient way in terms of accuracy, reliability and time.

Direct geo-referencing is used mainly when high accuracy is not needed, for example, in vegetation survey and carbon monitoring missions. Meter accuracy can be achieved when ordinary, non-RTK receivers are used while it can be improved to a couple of centimeters when RTK is applied. Similarly, the Inertial Navigation System (INS), as well as the Inertial Measurement Unit (IMU) plays an important role in a quality of a direct geo-referencing. Inertial Navigation System (INS) is equipped with motion sensors (accelerometers), rotation sensors (gyroscopes) and magnetometers and is responsible for collecting data about forces acting on the aircraft. There is also a barometer, which determines the actual altitude of UAV over

the starting point. They are essential for fixing UAV's position and providing the highest possible accuracy of a final ortho-photo product.

6.9.2 Self-Calibrating Bundle Adjustment: Structure from Motion

In order to relate the UAV image to a world coordinate system, knowledge for inner geometry and exterior orientation of the camera is needed. Exterior orientation establishes the position of the camera projection center in the ground coordinate system. This process is to relate image coordinates in the sensor plane (two dimensions based on central projection) to the object point in the ground coordinate system (in three dimensions). They can be achieved by two approaches: classical photogrammetric workflow or computer vision (CV) technique. However, the former approach is mostly applicable to high-level classical airborne photogrammetry since it relies on known camera positions based on field surveying. The use of computer vision software is an alternative technique to create 3D models from photographs that evolved considerably in recent years [13]. To acquire approximate EOE (Exterior Orientation Elements), namely position of camera when the image was taken, the measurements are performed during the flight by on-board equipment. This information greatly reduces computation time needed for image matching. Even UAV equipped with simple C/A (coarse) receiver and low-cost INS system provides data that can be advantageous and useful. The accuracy of this devices and final required accuracy determine how EOE can be further used in bundle block adjustment, either as approximate values or for direct georeferencing. This is called self-calibration or self-calibrating bundle adjustment. The whole process of determining camera parameters and 3D structure is called 'Structure from Motion (Fig. 6.18). This alternative is cost effective and easy, compared to rigorous photogrammetry. The technique also only requires a few control measurements and the processing is automated.

Computer vision software integrates state-of-the-art SfM (Structure from-Motion) algorithms to generate/reconstruct very dense and accurate point clouds from a series of overlapping photographs (Fig. 6.19) [15, 54, 55]. Instead of a single stereo pair, the SfM technique requires a series of overlapping photographs as input to feature extraction and 3D reconstruction algorithms [13]. Even if the coordinates of the photos are not accurate enough for Ground Control, it can be highly beneficial using them in computations. In the first step, when photos are aligned/matched to each other, this information can be applied and serve as additional data, so that the software knows on which pictures it should look for matches and which can be omitted. It can greatly improve performance and reduce time consumed for the process. The image stitching methods treat the world as planar and simply stitch the different images together by finding their relative positions [56].

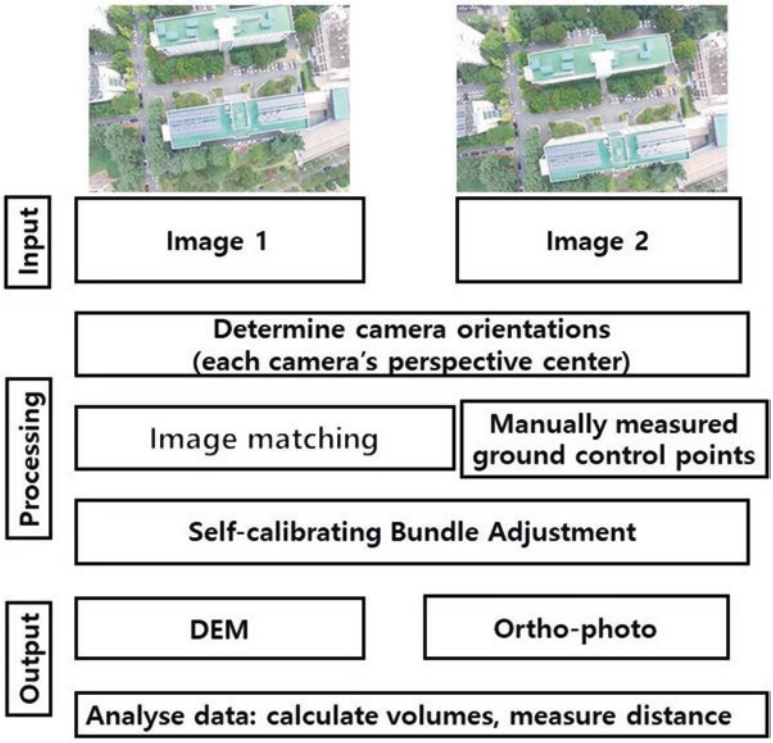

Fig. 6.18 Schematic representation of self-calibrating bundle adjustment through Structure from Motion

Various commercial software packages are available on the market, like Agisoft Photoscan, Pix4D Mapper and also open-source MicMac. They rely on tie point generated automatically based on feature-matching. The difference between classical photogrammetric approach and computer vision technique lies in fact that correspondences between images are computed automatically and the camera positions (Fig. 6.20) together with the scene structure are calculated simultaneously. They are usually obtained in an iterative bundle block adjustment that ensures statistically correct and robust solution. It is required that images are taken with sufficient overlap, so highly redundant number of connections is generated. However, there is also no need of using a metric camera, because its parameters are optimized during camera calibration procedure.

Agisoft PhotoScan is a stand-alone software package created and developed by Russian company founded in 2006. It can integrate vertical, oblique and motion imagery. PhotoScan imagery can both generated in controlled and uncontrolled situations with almost any camera ranging from low cost to highly professional medium-format cameras. It is designed to cope with photogrammetric computer vision projects such as area mapping or 3D object digitization task. Photoscan fol-

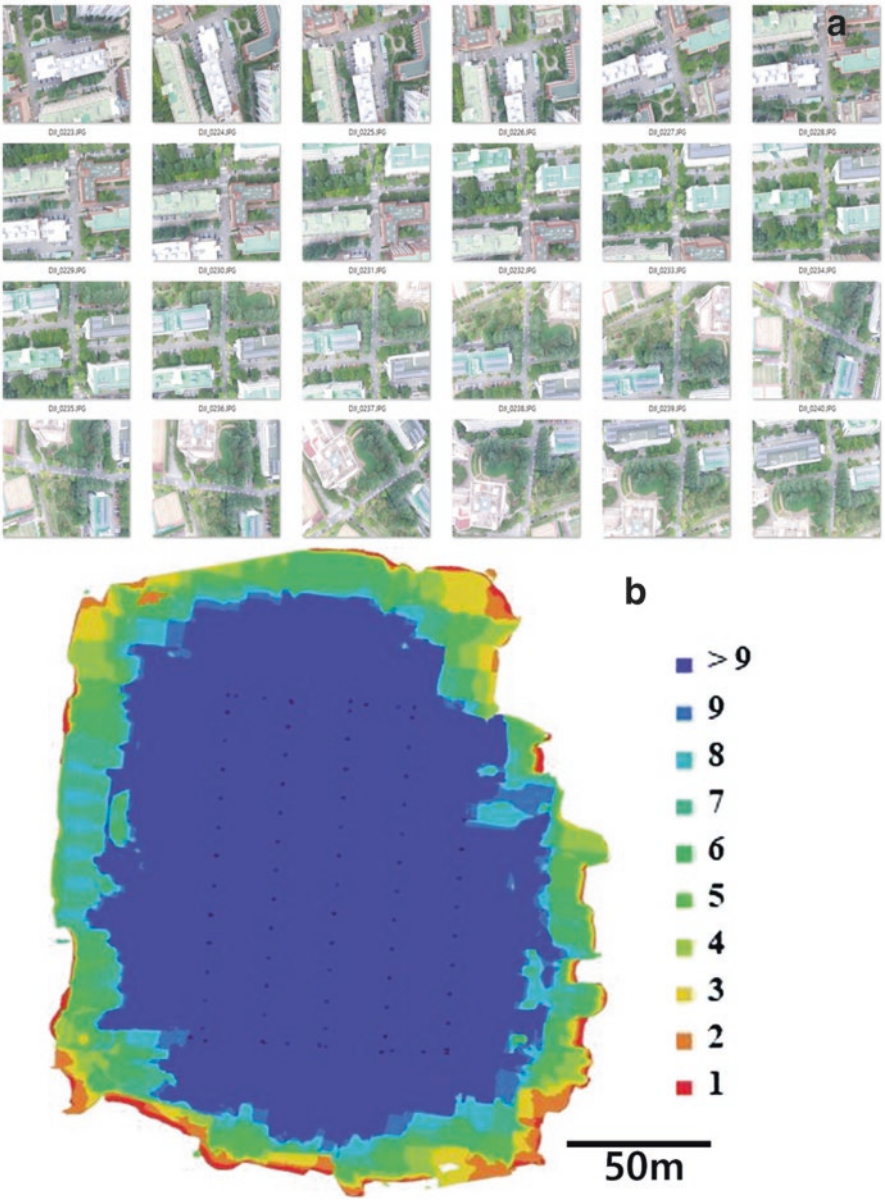

Fig. 6.19 Camera positions estimated using the scene structure of overlapping photographs, (**a**) 70% overlapped image taken from a different location (**b**) Camera locations and image overlap. Estimated camera locations are marked with a black dot. The overlapping of the photographs is displayed in color. The cooler color has a high degree of overlapping while warmer color represents a low degree of overlapping. Number of images (76), Flying altitude (100 m), Ground spatial resolution (3.61 cm/pixel)

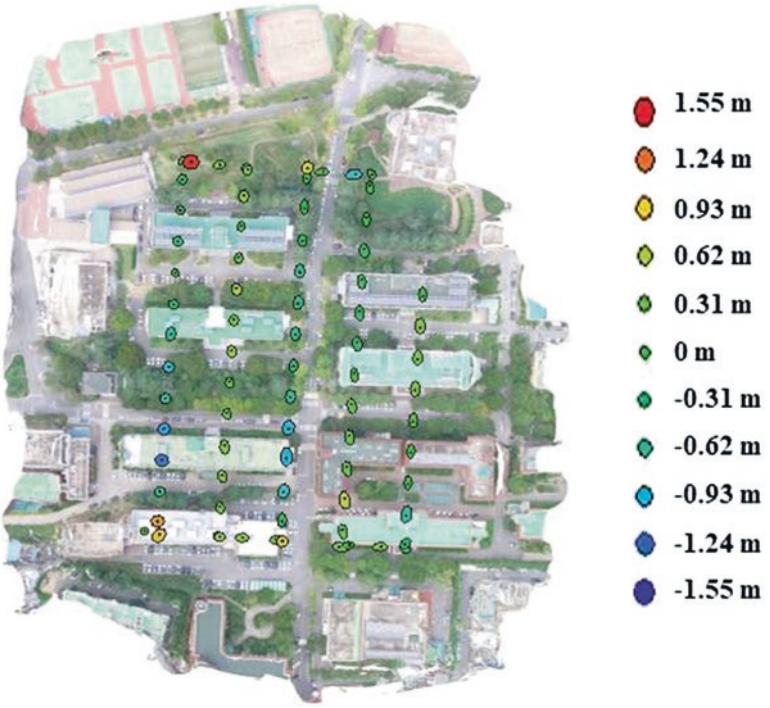

Fig. 6.20 Camera locations and error estimates. Z error is represented by ellipse color while X, Y errors are represented by ellipse shape. The error ellipse more circular, the more improved X, Y accuracy: Estimated camera locations are marked with a black dot. Average camera location error (m): X (0.473813), Y (1.24614), Z (0.51574), **Total (1.42946)**

lows a common SfM workflow through the steps of feature identification, matching and bundle adjustment to reconstruct the camera positions and terrain features as shown below:

1. Loading photos acquired into the PhotoScan software.
2. Inspection of loaded images and removal of unnecessary images
3. Alignment of the photos including the import of GCP

   Agisoft PhotoScan first carries out the automatic process of photo alignment by searching for common points on photographs. This alignment of the photos process starts with feature identification and image matching using the approximate GPS coordinates of the camera stations. Photoscan also performs automatic camera calibration as part of this step.
4. A sparse point cloud created through initial bundle adjustment

   Once photo alignment is completed, the software generates a sparse point cloud with a set of associated camera positions (orientation of each camera station), internal camera parameters, the XYZ/3D coordinates of all image features (tie points). A sparse point cloud is simply such a point cloud with relatively few

points. A sparse cloud may be adequate to produce a less detailed 3D model that doesn't need to be precisely georeferenced.

5. A dense point cloud set to high quality

   Agisoft PhotoScan requires this set of camera positions and an optimized sparse point cloud to advance in the process of producing a dense point cloud [51].

6. Next, the software builds a 3D polygonal "mesh" based on the dense point cloud, representing the surface of the object (a net drawn over a three-dimensional object).

   3D point clouds are mostly generated directly from stereo image matching, processing imagery algorithms by overlapping (terrestrial or airborne). This means that it is possible to acquire relevant ortho-mosaic parameters (camera location, overlap percentage, tie point coordinates) at low-cost, from 3D point cloud data [57, 58].

7. Builds texture over the 3D mesh, giving a sense of depth and volume.

   In the final step, the software lays texture taken from the original photographs over the 3D mesh, giving the original flat imagery a sense of depth and volume. The final outcome is a detailed 3D model (Fig. 6.21) that can be used for a variety of quantifiable or specialized analyses [51]. Finally, quality report is generated with information such as project summary, camera calibration details, accuracy of Ground Control Points and Check Points and other processing options. The ortho-mosaic generated from the drone imagery provides a high resolution visual summary of the target from a low altitude vantage point, revealing tiny details. The UAV-SfM approach offers economical alternatives to other traditional methods such as the ground control using Real Time Kinematic (RTK) GPS terrestrial surveys. The UAV-SfM approach plays an efficient role in rapidly producing

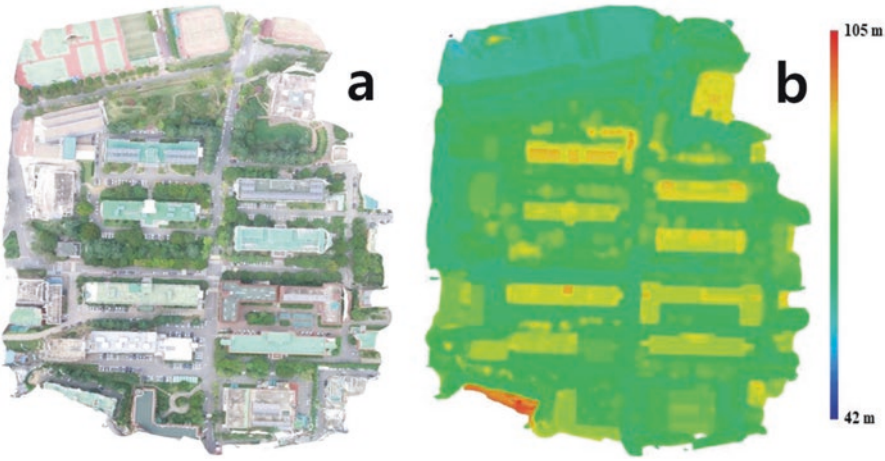

Fig. 6.21 Ortho-rectified imagery and 3D surface map, (**a**) Ortho-photo (**b**) Reconstructed digital elevation model (spatial resolution: 14.5 cm/pixel)

large-scale topography (higher temporal or spatial resolution) or detailed 3D models, practically on demand (high frequency). The spread of low-cost platforms combined with tiny MEMS cameras and GNSS systems offering point cloud coordinates constitutes some of the main characteristics for the success of this UAV-SfM technology [59].

6.10 Conclusion

The advancement and development of UAV imaging sensor technology over the last few years provided a considerable advantage of the current CPS framework in comparison to the traditional manned airborne sensor or in-situ survey for hyper-localized target. The narrow target requires extremely low-level flight and longer zoom lens, which almost inevitably result in serious image motion. Several previous studies based on manned aerial photography have noted the difficulty of obtaining large scale imagery free of image motion. This book emphasizes low-height drone photography (LHDP) based on lightweight and inexpensive smaller sensor (e.g. 10 mm) and platforms operated at relatively low height (100 m or so).

Off-the-shelf and low cost imaging sensor can provide centimeter-level spatial resolution imagery while location accuracy products of sub-meter level could be collected with low cost location sensor. In addition, the user can collect and process, very rapidly, realistic 3D data at a low cost, especially when compared with traditional methods. Computer vision based SfM allows the user to combine the virtual data to the real world, using UAV imageries. Each sensor type is being continually improved by combining infrared, and synthetic aperture radar to provide better spectral resolution in numerous applications.

Unmanned imaging sensors will be an area of both spatial resolution and spectral resolution evolution over the next 10–15 years [60]. The competition between USA and Russia to occupy the global leadership in space exploration was the driving force of the first remote sensing era. The remote sensing demand to obtain technological competitiveness in the global market such as a self-driving flying car is leading to the second remote sensing era. Popularized with the rapid development of location/imaging sensor and network technology, drone remote sensing will affect deeply our life style. In the near future drone remote sensing will become a necessity shooting and sharing aerial photographs in daily life of the general public (like current SMS, short message service).

References

1. Dickerson K (2015) Companies want to launch satellites that can see a phone in your hand from space. Business Insider
2. Bracher A, Sinnhuber BM (2009) An introduction to remote sensing. http://www.iup.uni-bremen.de/~bms/remote_sensing/remote_sensing_chap5.pdf. Accessed 30 Sept 2018

3. Natural Resources Canada (2015) Spatial resolution, pixel size, and scale. Natural Resources Canada. https://www.nrcan.gc.ca/node/9407. Accessed 22 Sept 2018
4. Strüder L, Davis JM, Hartman R, Holl P, Ihle S, Kalok D, Soltau H (2017) Spatial resolution smaller than the pixel size? Yes we can! Microsc Microanal 23(S1):90–91. https://doi.org/10.1017/S1431927617001131
5. A Canada Centre for Remote Sensing (2016) Tutorial: fundamentals of remote sensing. Natural Resources Canada. http://www.nrcan.gc.ca/sites/www.nrcan.gc.ca/files/earthsciences/pdf/resource/tutor/fundam/pdf/fundamentals_e.pdf. Accessed 30 Sept 2018
6. Mavi HS, Tupper GJ (2004) Agrometeorology: principles and applications of climate studies in agriculture. CRC Press, Boca Raton
7. Karpowicz J (2016) Figuring out aerial surveying with a Drone instead of arguing about photogrammetry vs LiDAR. Commercial UAV News. Diversified Communications, Free Street, Portland, ME
8. Veys C, Hibbert J, Davis P, Grieve B (2017) An ultra-low-cost active multispectral crop diagnostics device. In: SENSORS, 2017. IEEE, pp 1–3
9. Wikipedia (2018) Hyperspectral imaging. https://en.wikipedia.org/wiki/Hyperspectral_imaging. Accessed 30 Sept 2018
10. Smith RB (2012) Introduction to remote sensing of environment (RSE). MicroImages, Inc. http://www.microimages.com/documentation/Tutorials/introrse.pdf. Accessed 30 Sept 2018
11. Aber JS, Marzolff I, Ries JB (2010) Chapter 1 – introduction to small-format aerial photography. In: Aber JS, Marzolff I, Ries JB (eds) Small-format aerial photography. Elsevier, Amsterdam, pp 1–13. https://doi.org/10.1016/B978-0-444-53260-2.10001-8
12. Neumann KJ (2008) Trends for digital aerial mapping cameras. Int Arch Photogram Rem Sens Spatial Info Sci (ISPRS) 28:551–554
13. Boon MA, Greenfield R, Tesfamichael S (2016) Unmanned aerial vehicle (UAV) photogrammetry produces accurate high-resolution orthophotos, point clouds and surface models for mapping wetlands. S Afr J Geol 5(2):186–200
14. National Aeronautics and Space Administration (2018) Data processing levels. NASA. https://science.nasa.gov/earth-science/earth-science-data/data-processing-levels-for-eosdis-data-products/. Accessed 22 Sept 2018
15. Verhoeven G (2011) Taking computer vision aloft–archaeological three-dimensional reconstructions from aerial photographs with photoscan. Archaeol Prospect 18(1):67–73
16. Nogueira K, dos Santos JA, Cancian L, Borges BD, Silva TS, Morellato LP, Torres RdS (2017) Semantic segmentation of vegetation images acquired by unmanned aerial vehicles using an ensemble of ConvNets. In: Geoscience and remote sensing symposium (IGARSS), 2017 IEEE International, pp 3787–3790
17. Ammour N, Alhichri H, Bazi Y, Benjdira B, Alajlan N, Zuair M (2017) Deep learning approach for car detection in UAV imagery. Remote Sens 9(4):312
18. Crisp S (2013) Camera sensor size: why does it matter and exactly how big are they? New Atlas. GIZMAG PTY LTD 2018
19. Connor JO, Smith M (2016) Selecting cameras for UAV surveys. GIM Int 30:34–37. Geomares Publishing
20. Um J-S (1999) Airborne video as a remote sensor for linear target: academic research and field practice. Korean J Remote Sens 15(2):159–174
21. Um J-S, Wright R (2000) Effect of angular field of view of a video sensor on the image content in a strip target: the example of revegetation monitoring of a pipeline route. Int J Remote Sens 21(4):723–734
22. Um J-S, Wright R (1999) 'Video strip mapping (VSM)'for time-sequential monitoring of revegetation of a pipeline route. Geocarto Int 14(1):24–35
23. Um J-S, Wright R (1998) A comparative evaluation of video remote sensing and field survey for revegetation monitoring of a pipeline route. Sci Total Environ 215(3):189–207
24. Um J-S, Wright R (1996) Pipeline construction and reinstatement monitoring: current practice, limitations and the value of airborne videography. Sci Total Environ 186(3):221–230

25. Ramos TB, Caeiro S, de Melo JJ (2004) Environmental indicator frameworks to design and assess environmental monitoring programs. Impact Assess Project Apprais 22(1):47–62. https://doi.org/10.3152/147154604781766111
26. Caeiro S (2004) Environmental data management in the Sado estuary: weight of evidence to assess sediment quality. Universidade Nova de Lisboa
27. Akanmu A, Anumba C, Messner J (2014) Critical review of approaches to integrating virtual models and the physical construction. Int J Confl Manag 14(4):267–282. https://doi.org/10.1080/15623599.2014.972021
28. Aber JS, Aber SW, Pavri F (2002) Unmanned small format aerial photography from kites acquiring large-scale, high-resolution, multiview-angle imagery. Int Arch Photogramm Remote Sens Spat Inf Sci 34(1):1–6
29. Park S-I, Um J-S (2018) Differentiating carbon sinks versus sources on a university campus using synergistic UAV NIR and visible signatures. Environ Monit Assess 190(11):652. https://doi.org/10.1007/s10661-018-7003-x
30. Adão T, Hruška J, Pádua L, Bessa J, Peres E, Morais R, Sousa JJ (2017) Hyperspectral imaging: a review on UAV-based sensors, data processing and applications for agriculture and forestry. Remote Sens 9(11):1110
31. Keller J (2014) Infrared sensors blending with signal processing to yield new levels of surveillance. Military & Aerospace Electronics
32. Calderón R, Navas-Cortés J, Zarco-Tejada P (2015) Early detection and quantification of verticillium wilt in olive using hyperspectral and thermal imagery over large areas. Remote Sens 7(5):5584
33. Uto K, Seki H, Saito G, Kosugi Y (2013) Characterization of rice paddies by a UAV-mounted miniature hyperspectral sensor system. IEEE J Sel Top Appl Earth Obs Remote Sens 6(2):851–860. https://doi.org/10.1109/JSTARS.2013.2250921
34. Keller J (2012) Advanced military night-vision sensors rely on sensor fusion, networking, and signal processing. Military & Aerospace Electronics
35. Markus Melin ACS, Paul Glover-Kapfer (2017) Remote sensing: lidar. WWF Conservation Technology Series, United Kingdom
36. Lin Y, Hyyppa J, Jaakkola A (2011) Mini-UAV-borne LIDAR for fine-scale mapping. IEEE Geosci Remote Sens Lett 8(3):426–430
37. Agishev R, Comerón A (2018) Assessment of capabilities of lidar systems in day-and nighttime under different atmospheric and internal-noise conditions. In: EPJ Web of conferences. EDP Sciences, p 01018
38. Lefsky MA, Cohen WB, Parker GG, Harding DJ (2002) Lidar remote sensing for ecosystem studies lidar, an emerging remote sensing technology that directly measures the three-dimensional distribution of plant canopies, can accurately estimate vegetation structural attributes and should be of particular interest to forest, landscape, and global ecologists. Bioscience 52(1):19–30. https://doi.org/10.1641/0006-3568(2002)052[0019:LRSFES]2.0.CO;2
39. Chuvieco E, Vega JM (1990) Visual versus digital analysis for vegetation mapping: some examples on Central Spain. Geocarto Int 5(3):21–30. https://doi.org/10.1080/10106049009354265
40. Parasuraman R, Cosenzo KA, De Visser E (2009) Adaptive automation for human supervision of multiple uninhabited vehicles: effects on change detection, situation awareness, and mental workload. Mil Psychol 21(2):270–297
41. Cook KL (2017) An evaluation of the effectiveness of low-cost UAVs and structure from motion for geomorphic change detection. Geomorphology 278:195–208
42. Lucieer A, de Jong SM, Turner D (2014) Mapping landslide displacements using structure from motion (SfM) and image correlation of multi-temporal UAV photography. Prog Phys Geogr 38(1):97–116
43. Sui H, Tu J, Song Z, Chen G, Li Q (2014) A novel 3D building damage detection method using multiple overlapping UAV images. Int Arch Photogramm Remote Sens Spat Inf Sci 40(7):173

44. Chen B, Chen Z, Deng L, Duan Y, Zhou J (2016) Building change detection with RGB-D map generated from UAV images. Neurocomputing 208:350–364
45. Eisenbeiß H (2009) UAV photogrammetry. University of Technology Dresden
46. Schenk T (2005) Introduction to photogrammetry. The Ohio State University, Columbus. http://www.mat.uc.pt/~gil/downloads/IntroPhoto.pdf. Accessed 30 Sept 2018
47. Rossi P, Mancini F, Dubbini M, Mazzone F, Capra A (2017) Combining nadir and oblique UAV imagery to reconstruct quarry topography: methodology and feasibility analysis. Eur J Remote Sens 50(1):211–221. https://doi.org/10.1080/22797254.2017.1313097
48. Jiang S, Jiang W, Huang W, Yang L (2017) UAV-based oblique photogrammetry for outdoor data acquisition and offsite visual inspection of transmission line. Remote Sens 9(3):278
49. DJI (2015) Inspire 1 user manual V1.0
50. Um J-S (1997) Evaluating operational potential of video strip mapping in monitoring reinstatement of a pipeline route. University of Aberdeen, Aberdeen
51. Greenwood F (2015) How to make maps with drones. Drones and aerial observation, July, pp 35–47
52. Linder W (2009) Digital photogrammetry. Springer
53. Um J-S, Wright R (1999) Video strip mosaicking: a two-dimensional approach by convergent image bridging. Int J Remote Sens 20(10):2015–2032
54. Westoby MJ, Brasington J, Glasser NF, Hambrey MJ, Reynolds JM (2012) Structure-from-motion' photogrammetry: a low-cost, effective tool for geoscience applications. Geomorphology 179:300–314. https://doi.org/10.1016/j.geomorph.2012.08.021
55. James M, Robson S (2012) Straightforward reconstruction of 3D surfaces and topography with a camera: accuracy and geoscience application. J Geophys Res Earth Surf 117(F3):F03017
56. Vasisht D, Kapetanovic Z, Won J, Jin X, Chandra R, Sinha SN, Kapoor A, Sudarshan M, Stratman S (2017) FarmBeats: an IoT platform for data-driven agriculture. In: 14th USENIX symposium on networked systems design and implementation, Boston, MA, USA, 2017. USENIX Association, pp 515–529
57. Tenedório JA, Rebelo C, Estanqueiro R, Henriques CD, Marques L, Gonçalves JA (2016) New developments in geographical information technology for urban and spatial planning. In: Geospatial research: concepts, methodologies, tools, and applications. IGI Global, pp 1965–1997
58. Marques LFdESC (2017) Augmented valuation of cultural heritage through digital representation based upon geographic information technologies: the case study of Lisbon aqueduct system within an augmented reality environment. Universitat Politècnica de Catalunya, Portugal
59. Nex F, Remondino F (2014) UAV for 3D mapping applications: a review. Appl Geomatics 6(1):1–15
60. Howard C (2012) Unmanned, sensor-laden, and ubiquitous. Military & Aerospace Electronics. Military & Aerospace Electronics